scientific reports

OPEN

Energy analysis and feasibility of using solar energy in the novel hybrid system of a solar hot plate dryer in Iran

Kimia Taki, Bahram Hosseinzadeh Samani✉, Mahsa Forouzandeh & Zahra Shafiee

The drying process in agriculture is energy-intensive and traditionally relies on fossil fuels, which are becoming less reliable and more expensive. This study designed and simulated a hybrid solar hot plate dryer system using the computer to reduce reliance on fossil fuels. The system's main components are a flat plate collector, photovoltaic panels, and a wind turbine. This system was simulated in three cities of Iran, including Bushehr, Kerman, and Shahrekord, from May 22 to October 23. Results showed that Bushehr had the best wind turbine performance, producing 1.35×10^9 W annually. Shahrekord was ideal for solar energy, reaching solar radiation levels of about 4540 kJ/m²hr in September and generating 6660 W of solar-heated water. Finally, by comparing the yearly yield, it was concluded that Bushehr had a higher yield than the other two cities due to its geographical location, which was 0.301. The results of this research indicated that Iran, with its sunny days and wind energy potential, will be a very suitable place for installing and operating the hot plate solar dryer system. Future studies should look at longer-term simulations, use real-time data, and consider cost-benefit analyses to improve system efficiency and applicability.

Recently, energy consumption has also increased due to the modernization of people's lifestyles, the development of technology, and the growth of the world's population. For this reason, scientists and engineers focus on renewable energies to respond to this need and the limitation of fossil fuel resources[1]. Today, due to the reduction of fossil fuels, price fluctuations of these types of fuels, as well as environmental concerns, the potential of using solar energy, especially in the agricultural sector, has increased significantly[2]. The sun is the main source of free and inexhaustible energy for Earth. Solar energy can be a very good source of energy for future generations. One of the advantages of using this energy is that it is the most abundant, reliable, accessible, and compatible renewable energy source.

Every year, about four million exajoules (each exajoule equal to 1018 joules) of solar energy reach the Earth, which can be easily harvested and used. Studies have shown that it is possible to respond to the increasing global demand for energy by using solar energy[3,4]. A lot of research has been done in the field of using solar energy in different industries. In the research conducted by Parsa et al. in 2020, solar energy was used for the solar water disinfection system (SODIS). Finally, they reported that using silver nanoparticles for dual purposes (antibacterial and heat/mass transfer enhancement) and exposing distilled water to sunlight for SODIS could result in healthier water[5].

Salem et al. used the solar system to produce hydrogen in another study. The system comprises main components: a PV array, an electrolyzer, a fuel cell, a battery, a hydrogen storage unit and a controller in the complete loop. The hydrogen cogeneration system results provide 7.8% efficiency in the cold climate of Fargo, North Dakota, due to lower solar insolation. The hot climate condition of Lahore weather provides an efficiency of 11.8%, which satisfies the statistics found in the literature[1]. Also, in the research conducted by Alsehli et al. in 2022 on the desalination of water by the solar system, it was found that this method is an effective and efficient method for water desalination, and the components of this system consist of a modified solar still (MSS), parabolic trough solar collector (PTSC), separation unit (SU), and two external condensers (EC)[6]. Therefore, as it was clear, according to previous research, solar energy has been widely used since ancient times and has been the basis of many researches and discoveries.

Department of Mechanical Engineering of biosystem, Shahrekord University, Shahrekord, Iran. ✉email: b.hosseinzadehsamani@gmail.com

1

Solar energy is used in photovoltaic panels, water heating, and solar thermal systems in various fields, such as electricity generation, hot water supply, heating and cooling systems, and drying processes in the agricultural industry. One of the important processes of post-harvesting in agriculture is the drying process. In terms of energy consumption, this process is considered one of the most intensive post-harvest processes. Drying is one of the most important processes in protecting and increasing the shelf life of agricultural products. Also, the drying process increases product quality, reduces transportation costs, and reduces post-harvest losses[7–9].

In drying, moisture is partially removed from an agricultural product to reach the standard moisture level[10,11]. This operation is done using different methods, such as drying by direct exposure to the sun (open sun drying), solar drying, and mechanized drying. In the traditional drying method, which is the simplest and cheapest, the product is often placed in the open air on the ground and exposed to sunlight. One of the disadvantages of this method is food exposure to rain, dust, and pollution. This method does not control the drying process, and exposure to direct sunlight is undesirable for some agricultural products and food. Another disadvantage of this method is the attack on insects, animals, and birds[12]. With the development of industry and agriculture, mechanized drying is one of the methods that have been proposed, but it should be considered that these methods are very expensive and have high energy consumption. Also, in some of these dryers, the drying rate is low[13]. Therefore, according to the disadvantages of these dryers, it is preferable to use solar dryers.

In solar dryers, sunlight is absorbed by collectors, and the resulting heat is transferred to the dryer chamber through a fluid, and the drying process takes place. Solar dryers are cheap, safe methods that offer good quality and minimal environmental impact. Solar dryers are available in different sizes and types. These dryers are generally divided into four categories: direct solar dryers, indirect solar dryers and hybrid solar dryers[14–16]. Direct solar dryers are a good alternative to drying by exposure to sunlight (open sun dryers). These dryers have an insulated chamber, a box that often has a transparent glass cover is used to prevent heat loss and protect the product from dust and insect attacks. When the sun shines on the glass cover, some of the radiation is absorbed and heats the air. Then, the heated air circulates naturally or with the help of an external source, such as a blower or a fan inside the chamber, and the moisture evaporates from the surface of the material. The other part of the sun's radiation is reflected. These dryers have a simple design, are usually cheap, and are mostly used in areas that have sunlight for a long time during the day. Another important point is that this dry type protects the product from wind, rain, pollution, and insect attacks[17]. But the disadvantage of these dryers is that they have a limited capacity, and their final product doesn't have high quality[7,14].

In another type of solar dryer, which is called the indirect dryer, the dryer chamber is a separate unit in such a way that the solar collectors first absorb the sun's radiations. The fluid used (water or air) heats, then the heated fluid enters the drying chamber, and the drying process of the product takes place from the heat of the fluid. This type of dryer performs much better than other dryers and has solved many problems in the drying process, such as energy balance. In fact, if the design of this type of dryer is principled and correct, it is possible to achieve optimal temperature values, optimal air flow rate, high performance, good quality of the manufactured product, and shortening the drying process time[18,19]. A study conducted by Khalil et al. (2023), provided a comprehensive review in detail of the most important and latest technologies that have been combined with solar dryers, which showed a significant improvement in the performance of solar dryers[20].

In hybrid dryers, for temperature stability, in addition to the main source of heat, sunlight, another auxiliary source is used, providing the necessary energy from burning biogas or an electricity source. In fact, in these dryers, an auxiliary source is mostly used for fluid preheating[21]. In recent years, much research related to the current research has been done for example in a research conducted by Ahmadi et al. (2021), agro-product drying technologies powered by solar energy were presented and discussed. Different types of solar dryers based on direct, indirect and mixed modes were described. And, energy, exergy, economic, and environmental analyses for these technologies were presented. The results indicated that the air mass flow rate, temperature, moisture content, and drying time are the most important parameters in solar dryer performance[22]. In another study by philip et al. (2022) focuses on benefits of solar drying over open sun drying, in this research the development and analysis of a 100 kg capacity greenhouse solar dryer was designed to produced high-quality dried products. According to annualized cost method calculations, the cost of drying products by using a solar dryer is less than electric dryer[23]. Therefore, according to the previous studies and also the deficiencies that exist in each of them, This study presents a new type of solar hot plate dryer that combines several renewable energy sources such as, solar energy, wind energy, and photovoltaic panels into one system specifically designed for agricultural use in different cities of Iran. Unlike previous systems that rely on just one energy source, this hybrid design adjusts energy use based on available sources (sunlight or wind). Additionally, the system is modeled using computer simulations that account for different climates in various cities in Iran, making it more efficient and adaptable than traditional solar dryers. This innovative approach significantly improves upon existing technologies by using a diverse mix of energy sources tailored to specific conditions.

Materials and methods
Setting up the solar hot plate drying system
This system consists of a hot plate dryer; a complete solar system provides the energy required for this system. In order to supply the required heat for the dryer, a solar water heating system has been used, and the electrical energy used in this system was supplied from photovoltaic panels and wind energy. The simulation of this system was done using writing code on a computer, which was based on weather information obtained from Iranian Meteorological Organization for the three cities of Shahrekord, Kerman, and Bushehr.

Figure (1) shows that this system consists of a hot plate dryer, pipe, pump, tank, controller, flat plate collector, photovoltaic panel, and wind turbine.
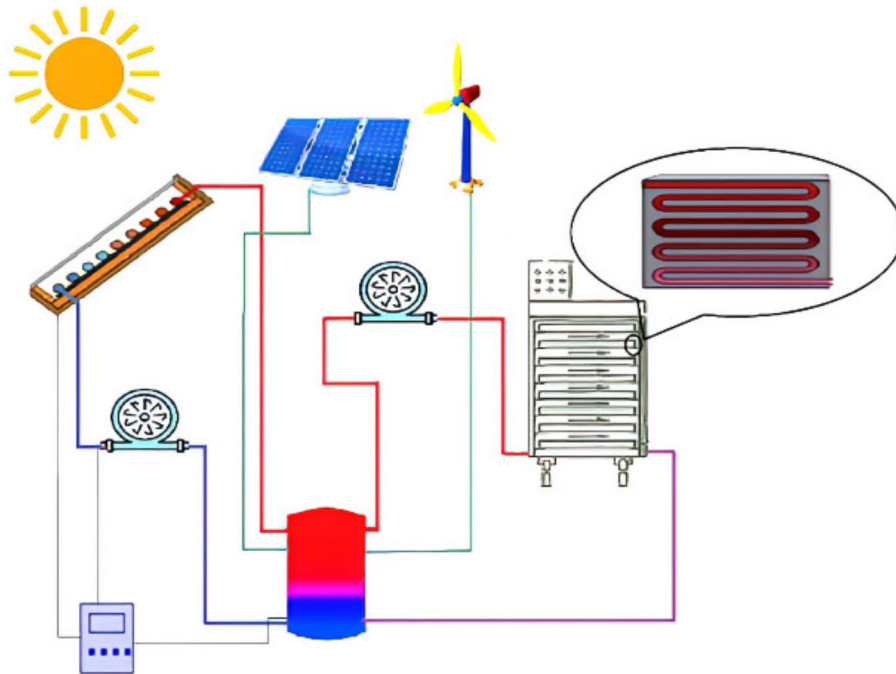
Fig. 1. Schematic of solar hot plate dryer.

Hot plate dryer

Hot plate dryers consist of a metal plate with a flat surface. Food and agricultural products are placed on this surface. This plate is heated with the help of the fluid flow inside the pipes located under the dryer plate. Then, as the plate heats up, the moisture is separated from the product, and the product gradually dries. An airflow system is also created around the hot plate so that the steam resulting from the evaporation of food moisture is quickly absorbed, and the drying process is carried out more effectively. This research used three hot plate dryers, each consisting of 20 and 60 trays. In order to supply heat to the plates, pipes are installed under each plate to establish the flow of hot water heated by the solar collector and stored in the tank under the plates. The heat is transferred to the plates by the water through the pipes, and they become hot, and the drying process takes place. The pipes used in this research were made of copper with a length of 200 m and an inner diameter of 1 cm with a heat loss coefficient of 13.14 w/m²k.

Simulation of the solar system

To analyze the performance of the solar dryer system, the system was simulated in computer. As shown in Fig. (2), this simulated system a includes two parts for supplying thermal energy for the dryer, which includes the solar water heating and its related components, and the other part of the system, which is used to provide electrical energy, include wind turbine and photovoltaic panels. The following will introduce the components used in this system and their equations.

Introducing the type and model of components

Weather data processor
In order to analyze the performance of this system, three cities with different climates were selected in Iran. To obtain information and weather data of the three cities of Shahrekord (50.9 ˚E and 32.3 ˚N), Kerman (30.3 ˚N, 57.0 ˚E) and Bushehr (29.0 ˚N, 50.9 ˚E) from the information component Weather was used. Since the main activity of dried fruit factories is in summer to autumn, this simulation was done from May 22 to October 23. That is, from the 3384th hour to the 7080th hour. The time steps used are considered to be less than one hour, and in this research, a time step of 30 min has been set. This component provides useful information such as the ambient temperature, the amount of radiation, the amount of reflected radiation, and the angle of incidence for the surface of the collector. Table (1) shows some information necessary to complete the simulation.

Wind turbine
The drying process is one of the post-harvest technologies that requires a lot of energy. A wind turbine was used to supply the energy needed for this system. According to the selected type of turbine, the height of the hub for this turbine is 4 m. The turbine's power output is also obtained from Eq. (1).
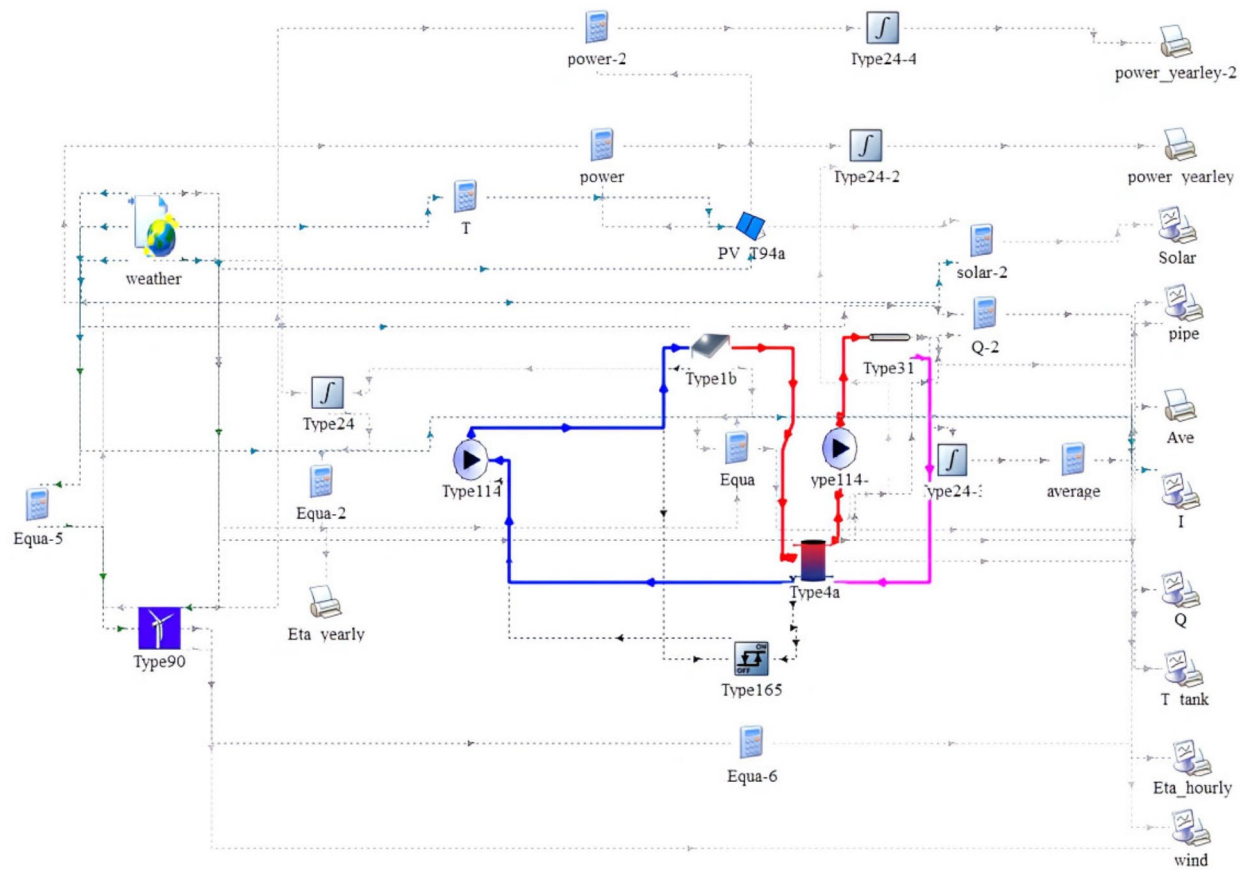
$$P = CP_{\rho} A_R U_0^3 \tag{1}$$

Fig. 2. Solar system simulation in computer.

Tilted Surface Radiation Mode	3	-
Ground reflectance - no snow	0.2	-
Ground reflectance - snow cover	0.7	-
Number of surfaces	1	-
Tracking mode	1	-
Slope of surface	40	Degrees
Azimuth of surface	0	Degrees

Table 1. Necessary information to complete the weather data component.

Site elevation	2100	m
Data collection height	3	m
Number of turbines	1	-

Table 2. Wind turbine module parameters.

In this equation, ρ is the air density (kg/m³), U_0 is the wind speed (m/s), A_R is the rotor area (m²), and Cp is a function of the axial induction coefficient[24]. Table (2) shows a number of parameters used in completing the simulation information.

Photovoltaic panel
Another main component in providing energy consumption for this system is photovoltaic panels. In fact, photovoltaic panels convert the energy of the sun's photons into the electrical energy required by this system. The module area is 0.89 m², and number of cells wired in series is 36. Also, 10 panels in parallel and 10 panels

Temperature coeficient of Isc	0.002	-
Temperature coeficient of Voc	-0.079	-
Number of cells wired in series	36	-
Module series resistance	-1	-
Module short-circuit current at reference conditions	6.5	amperes
Module open-circuit voltage at reference conditions	21.6	V
Module voltage at max power point and reference conditions	17	V
Module current at max PowerPoint and reference conditions	5.9	amperes

Table 3. Parameters of photovoltaic panel.

Number in series	1	-
Intercept efficiency	0.80	-
Efficiency slope	13.0	kJ/hr.m^2.K
Efficiency curvature	0.05	kJ/hr.m^2.K^2

Table 4. Flat plate collector parameters.

Tank loss coefficient	3.00	-
Height of nodes 1 to 5	0.05	M
Set point temperature for element 1	55	˚C
Deadband for heating element 1	5	˚C
Node containing heating element 2	1	-

Table 5. Parameters of tank component.

in series were considered for setting up this system. Other necessary information to complete the simulation is written in Table (3).

Flat plate collector
In this research, a collector with an area of 2 m^2 and an inlet flow rate of 100 kg/hr was considered. Other information about the flat plate collector component is given in Table (4).

The useful energy the flat plate solar collector collects is obtained from the Hottel-Whillier Eq. (2).

$$Qu = \dot{m}_f Cp_f (T_i - T_a) \tag{2}$$

ΔT represents the difference between the inlet temperature of the collector (Ti) and the ambient temperature (Ta), but according to the collector test report, sometimes the efficiency curve is presented according to the average temperature (Tave) or the outlet temperature (To), Eq. (3)[25].

$$\begin{aligned} \Delta Ti &= Ti - Ta \\ \Delta Tave &= Tave - Ta \\ Tave &= ((Ti - To)/2) \\ \Delta To &= To - Ta \end{aligned} \tag{3}$$

The efficiency of the flat plate solar collector is also obtained from the Eq. 4[26].

$$\eta = \frac{Qu}{A * IT} = a_0 - a_1 \frac{\Delta T}{IT} - a_2 \frac{(\Delta T)^2}{IT} \tag{4}$$

Where A is the Total collector array aperture or gross area (m^2), IT is the Global radiation incident on the solar collector (kJ/h-m^2), and a0, a1 and a2 are the maximum of the collector efficiency, Negative of the first-order order coefficient in collector efficiency equation (kJ/h-m^2-K) and second order coefficient in collector efficiency equation (kJ/h-m^2-K^2), respectively.

Tank
The water storage tank used in this research is Type 4a. This tank has a capacity of 500 L and has 5 nodes. Cold water enters the tank from the lowest node, and hot water leaves from the highest node. The temperature of the cold part of the tank was set at 22 ˚C, and the temperature of the upper or warm part of the tank was set at 45 ˚C. Also, as an auxiliary source, a heating element was placed in the upper part of the tank. Other information about the tank is given in Table (5).

Pump

In order to establish the flow of hot water between the tank and the collector, a type 114 pump, which is a single (constant) speed pump, was used to keep the fluid output mass flow constant. The rated flow rate of this pump was 1000 kg/hr, and its input flow rate was considered 200 kg/hr. According to Eq. (5), the pump motor's overall pump efficiency and efficiency are used to calculate the efficiency of the pumping process.

$$\eta_{pumping} = \frac{\eta \; overall}{\eta \; motor} \tag{5}$$

Where $\eta_{pumping}$ is the efficiency of pumping the fluid (0…1), $\eta \; overall$ is overall pump efficiency (motor efficiency * pumping efficiency) (0…1) and $\eta \; motor$ pump motor efficiency (0…1).

The power required in the pump shaft (excluding motor efficiency effects) was calculated according to Eq. (6).

$$P_{shaft} = P_{rated}\eta_{motor} \tag{6}$$

Where P_{shaft} is shaft power required by the pumping process (does not include motor in efficiency) (kJ/hr), P_{rated} is rated power of the pump (kJ/hr), and η_{motor} is pump motor efficiency (0…1).

The energy transferred from the pump motor to the fluid flow is calculated as Eq. (7).

$$Q_{fluid} = P_{shaft}(1 - \eta_{pumping} + (P - P_{shaft})f_{motorloss} \tag{7}$$

Where Q_{fluid} is energy transferred from the pump motor to the fluid stream passing through the pump (kJ/hr), and $f_{motorloss}$ is the fraction of pump motor inefficiencies that contribute to a temperature rise in the fluid stream passing through the pump (0…1)[27].

Controller

The controller has two states, 0 and 1, which indicate the on and off states. When the controller turns off, it means that because the temperature of the outlet of the collector is lower than the temperature of the inlet to the collector, water is not pumped from the tank to the collector, and it gives the order to turn on the auxiliary system (element of the tank). When the pump is working, the outlet temperature from the collector is higher than the inlet temperature of the collector. This research used a type 165 controller, and the number of oscillations and high-limit cut-outs were considered 5 and 100, respectively. This mathematical function is expressed according to Eqs. (8) and (9).

If the controller is on ($\Upsilon i = 1$):

$$\begin{aligned} &\text{If } \Delta T_L \leq (T_H - T_L) \text{ Then } \gamma_0 = 1 \\ &\text{If } \Delta T_L > (T_H - T_L) \text{ Then } \gamma_0 = 0 \end{aligned} \tag{8}$$

If the controller is off ($\Upsilon i = 0$):

$$\begin{aligned} &\text{If } \Delta T_H \leq (T_H - T_L) \text{ Then } \gamma_0 = 1 \\ &\text{If } \Delta T_H > (T_H - T_L) \text{ Then } \gamma_0 = 0 \end{aligned} \tag{9}$$

Where ΔT_H is upper dead band temperature difference (˚C), ΔT_L lower dead band temperature difference (˚C), T_H is upper Input temperature (˚C) and T_L is lower Input temperature (˚C)[28].

Figure (3) shows the function of the controller.

Pipe

In order to provide the necessary heat for the drying process, hot water was transferred to the dryer plate through pipes. Type 31 pipes were used in this research. The pipes were made of copper with a length of 200 m and a heat loss coefficient of 13.14 w/m²k. The reason for choosing copper pipes in this research was their high thermal conductivity, which made good heat transfer from hot water to dryer plates. Copper pipes are usually used in applications that require fast and efficient heat distribution[29]. The internal energy changes inside the pipe from the beginning of the simulation are obtained from Eq. (10).

$$\Delta E = MC_p(\bar{T}f - TI) \tag{10}$$

Where ΔE is the change in internal energy of fluid inside the pipe (kJ), M the mass of the fluid inside the pipe (kg), Cp the specific heat of the fluid (kJ/kg.K), $\bar{T}f$ the secondary temperature of the fluid (temperature of the fluid exiting the tube) (˚C) and TI is the initial temperature of the fluid or the temperature of the fluid entering the pipe (˚C)[30]. Other information about the pipe is given in Table (6).

Results and discussion

Considering that the drying process is one of the most energy-consuming technologies in agricultural post-harvesting, a complete solar system was used to perform this process. Also, considering that the main activity of dried fruit factories is in summer to autumn, this simulation was done from May 22 to October 23. The time steps for this simulation were set to 30 min, and the simulated system was tested for the three cities of Shahrekord, Kerman, and Bushehr, with different climates. In this section, the simulation results performed in computer to determine the relationship between solar radiation and the outputs of the proposed system are examined, analyzed, and compared.
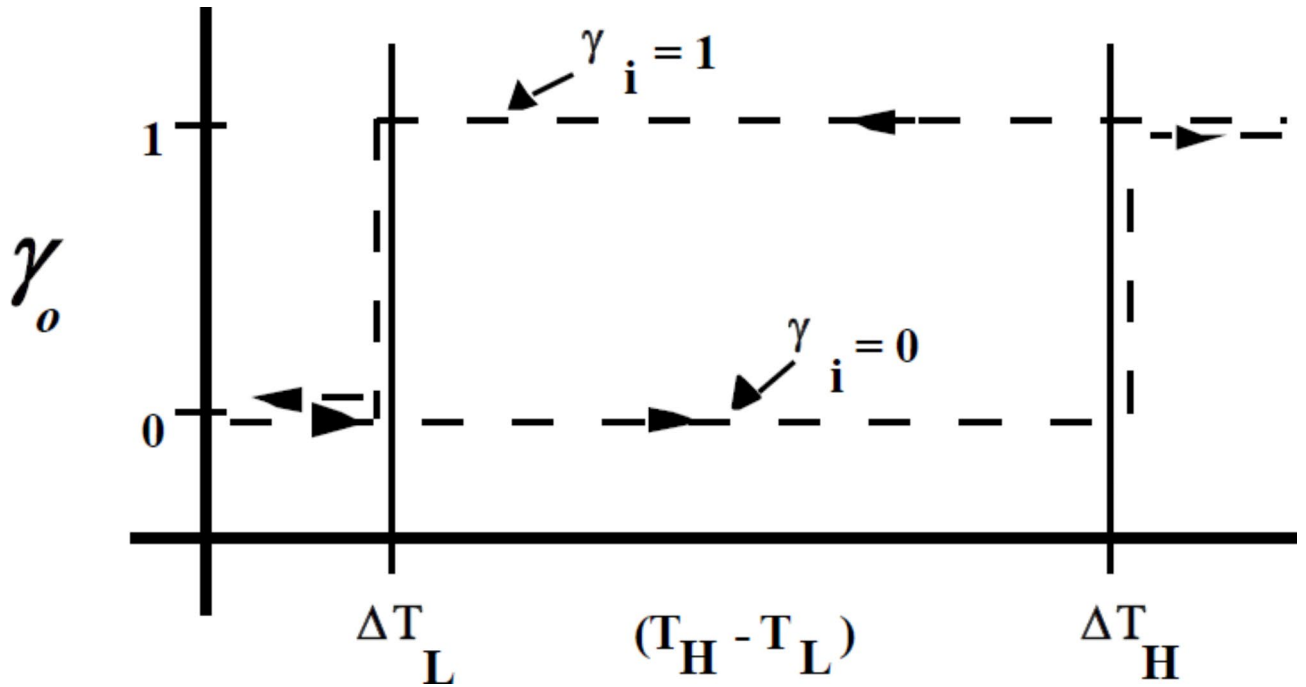
Fig. 3. The function of the controller.

Inside diameter	1	Cm
Initial fluid temperature	24	˚C
Fluid specific heat	1000	kJ/kg.K

Table 6. Pipe module parameters.

Amount of total radiation of the sun

In Figs. (4), (5), and (6), the amount of radiation (IT) that reaches the Earth's surface from the sun during the specified days is shown in three cities of Bushehr, Kerman, and Shahrekord. Based on the data obtained from these graphs, the maximum radiation and the best place to perform the drying process can be determined. According to diagram (4), the maximum amount of radiation for the city of Shahrekord was 6320 h, equivalent to the end of September (September 20), and was around 4540 kJ/m²hr. Also, according to the graph of Kerman city, the highest amount of radiation is 4410, which happened at 6300 h, equivalent to the end of September. Based on the diagram of Bushehr city, it can be concluded that the maximum amount of radiation in this city is around 3820, which happened at 6730, which is equivalent to the beginning of October.

From the comparison of the graphs and data obtained, also considering the location of Shahrekord, which is located in the foothills of the Zagros mountains and considering the height of this city above sea level and also considering that the Psh of this city compared to the other two cities are more, have the highest amount of radiation, and in terms of radiation potential, it is the best place to install and operate the desired system. As[31] reported, a lot of solar energy is available in most regions of Iran, especially its southern and central parts. They also claimed that if solar collectors are installed in only 1% of Iran's deserts, the energy produced will be 5 times more than the country's gross electricity production.

In another study conducted by[32] on the study of the solar energy potential of Iran, it was pointed out that Iran is a country with a different climate and has more than 300 sunny days, so it is an option, and it is considered as a good place for solar energy projects.

[33] Investigated the potential of different regions of Iran for building solar powerhouses; the results of their research showed that Iran has a very good potential for using solar power and can reduce the consumption of fossil fuels and the emission of CO_2 gas. Also, according to their research, it was found that the cities of Bandar Abbas, Bushehr, Isfahan, Kerman, Shiraz, and Yazd have a very good potential for building solar powerhouses compared to other regions.

Solar water heating performance

Figures (7) and (8) show the performance of the solar water heating system in the three cities of Bushehr, Kerman, and Shahrekord. The overall performance of this system can be checked by checking the performance of the solar collector and the auxiliary system in the tank. Diagram (7) shows the amount of useful energy
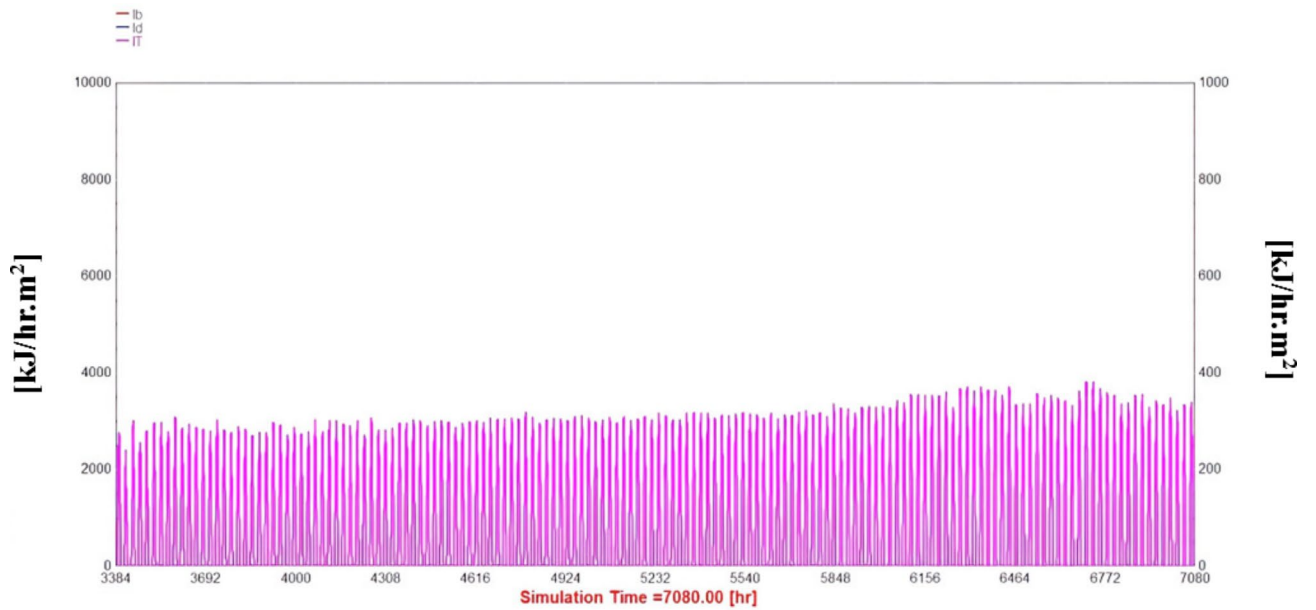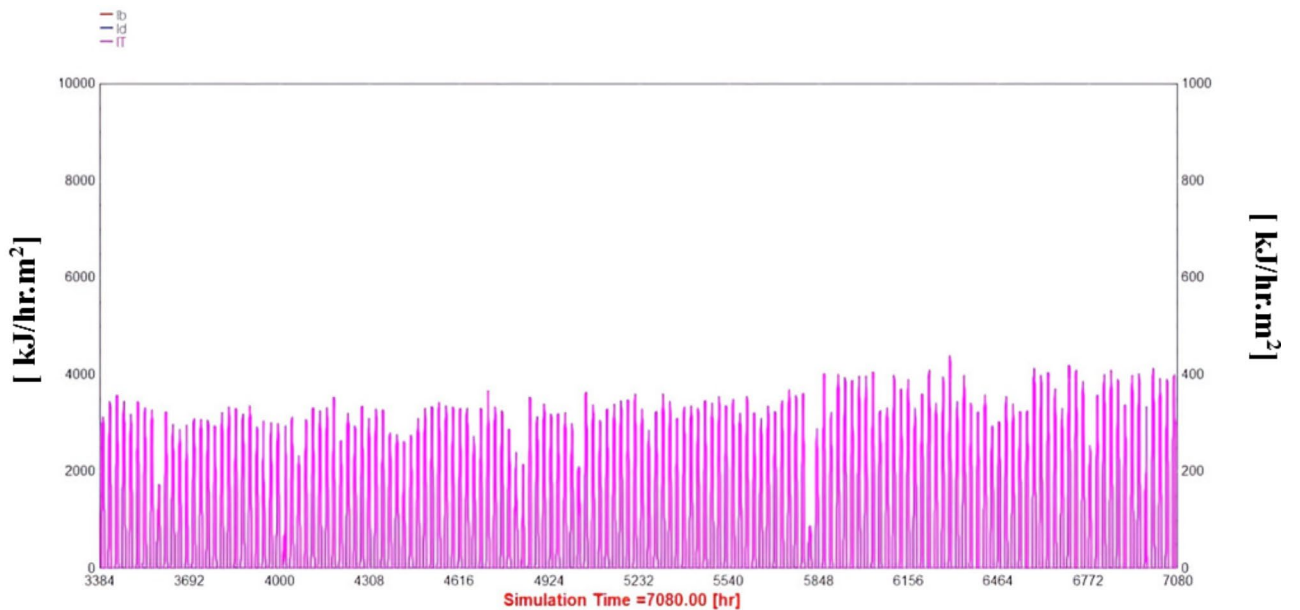
Fig. 4. Radiation diagram (IT) of Bushehr city.

Fig. 5. Radiation diagram (IT) of Kerman city.

produced by the solar collector (Qu) and the amount of energy required to supply heat to the dryer (Ql). Also, graph (8) shows the auxiliary system's energy demand (Qaux).

By analyzing the results, it can be concluded that the amount of useful energy produced by the solar collector is inversely proportional to the energy demand of the auxiliary system, while the amount of energy required to supply the domestic hot water load is almost constant. The maximum amount of useful energy the solar collector produces for Bushehr, Kerman, and Shahrekord is 5660 kJ, 6420 W, and 6660 W, respectively. It can be concluded that the solar collector had the best performance in Shahrekord and the lowest performance in Bushehr compared to the other two cities.

Also, by examining the Q_U diagram in Shahrekord, it is clear that the highest amount of useful energy produced by the solar collector in Shahrekord occurred in September. On the other hand, by examining the Qaux diagram in all three cities, it can be concluded that the maximum energy demand of the auxiliary system for all three cities was 14,400 W, which was for Bushehr and Kerman in September and for Shahrekord city in July.
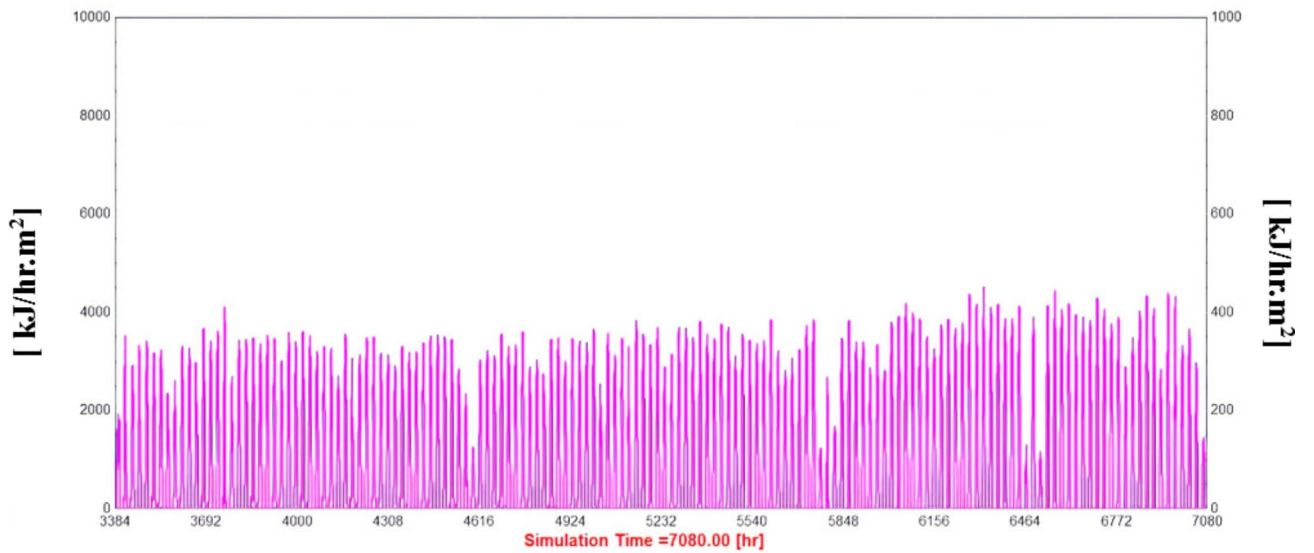
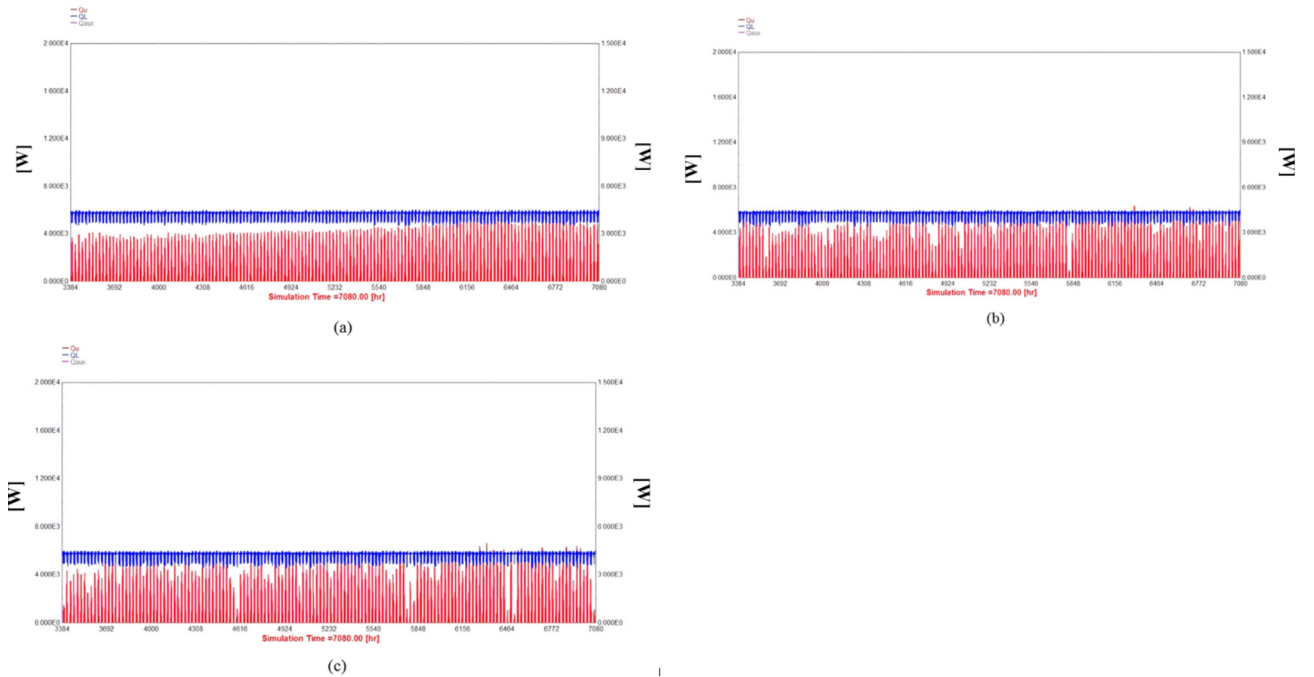**Fig. 6**. Radiation diagram (IT) of Shahrekord city.

Fig. 7. Diagram of useful energy produced and required energy of the dryer. (**a**) Bushehr (**b**) Kerman (**c**) Shahrekord.

Also, according to the graph, it is clear that the auxiliary system is off in all three cities from the end of September to October, which is a favourable time because it indicates that the amount of radiation to the surface of the solar collector is sufficient. It shows that the solar collector has the ability to produce the necessary energy to supply the heat needed by the dryer and does not need the auxiliary system to be on. In research conducted by[34], it was reported that due to the location of Iran, which is located at 25 to 40 degrees latitude, and also because Iran is on the list of top countries in the world in terms of receiving solar energy, it has a very good potential for using solar energy resources. In this research, several cities in Iran were selected to establish a solar water heating system, and the results showed that the central and southern cities of Iran performed better. Also, the city of Shahrekord was introduced as one of the very good options for creating and setting up a solar water heating system.
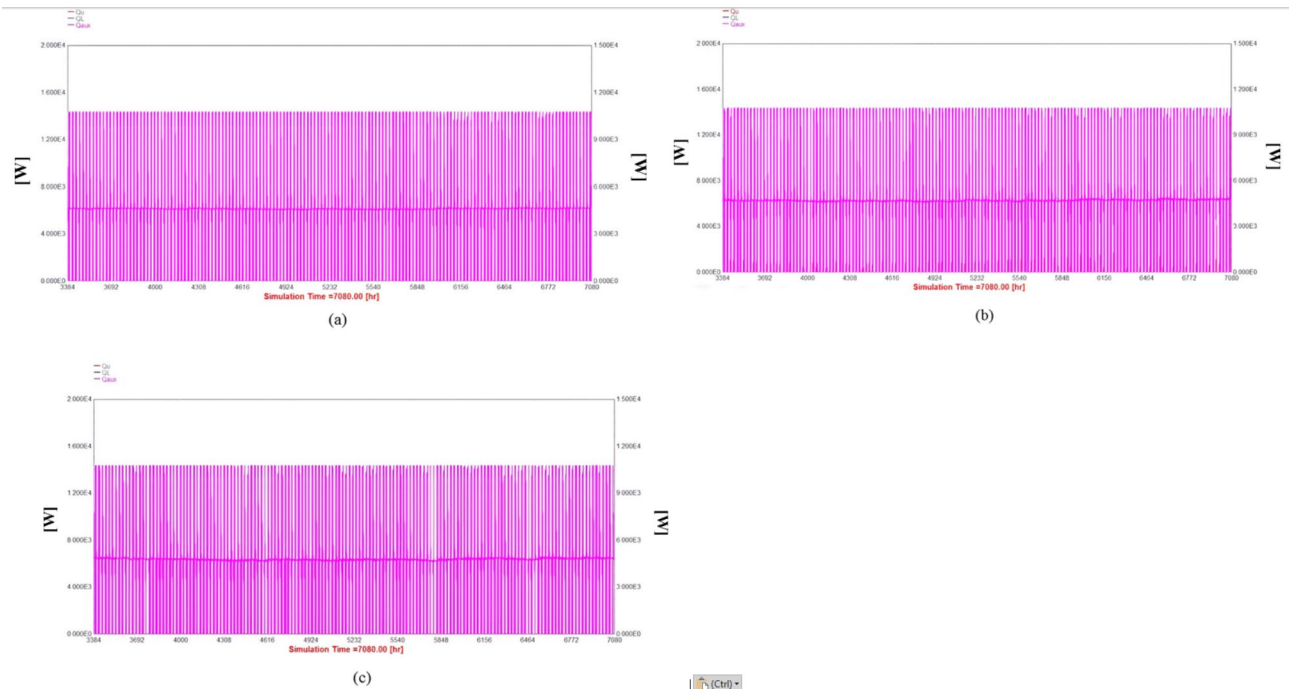
Fig. 8. Diagram of the required energy of the auxiliary system (**a**) Bushehr (**b**) Kerman (**c**) Shahrekord.

Photovoltaic panel performance

A very important component that plays a significant role in this solar system is the photovoltaic panel. This section aims to check the performance of this part of the system. Figure (9) shows the performance of the photovoltaic panel in Bushehr city.

Diagram (9a) shows the amount of radiation to the surface of the photovoltaic panel in Bushehr, and diagram (9b) shows the amount of power produced by the photovoltaic panel in this city on the specified date. As it is clear from this graph, the highest amount of radiation to the surface of the photovoltaic panel in this city was about 985 kJ/hrm^2, which happened in the summer season and in July. Also, the maximum power produced by the photovoltaic panel happened in the autumn season and in the month of October, and its value was equal to 31,100 kJ/hr.

Figure (10) shows the amount of radiation on the photovoltaic panel's surface and its production power in Kerman City. According to this diagram, the maximum radiation and power of this part of the solar system is equal to 1150 kJ/hr.m^2 and 36,100 kJ/hr, which happened in July and late summer in September.

Also, Fig. (11) indicates that in Shahrekord, the maximum radiation and power were 1270 kJ/hr·m^2 and 38,300 kJ/hr, respectively, recorded in June and October. The performance analysis of photovoltaic panels in these three cities shows that Shahrekord outperforms the others in terms of both absorbed radiation and produced power. This superior performance can be attributed to the geographical location of Shahrekord and its altitude above sea level, which provides more sunlight hours due to a higher peak radiation angle.

Shahrekord's continental climate also contributes to its high solar radiation levels, making it an optimal location for solar energy systems. Additionally, Shahrekord's climate, with lower humidity and fewer cloudy days, enhances solar panel efficiency. Comparing these results with other studies, [35] and [36] reported that higher altitudes and clear climates significantly improve PV panel performance. Akikur et al. found that PV systems in high-altitude regions of Nepal exhibited up to 20% higher efficiency compared to low-altitude areas due to reduced atmospheric scattering. Similarly, Hasanuzzaman et al. observed that clear skies and lower humidity in desert regions of Saudi Arabia resulted in higher PV panel output.

Wind turbine performance

A wind turbine was one of the components of this system, and it was used to supply the energy needed by the auxiliary system. Figure (12) shows the amount of power produced and the efficiency of wind turbines in the three cities of Bushehr, Kerman, and Shahrekord. According to the graph of Bushehr city (Fig. 12a), the maximum power produced by the turbine in this city is 4.86×10^6 W, and the highest efficiency of the turbine in this city is about 0.468, which happened at the end of October. Also, when the turbine had the highest efficiency, its production power was around 31.2×10^6.
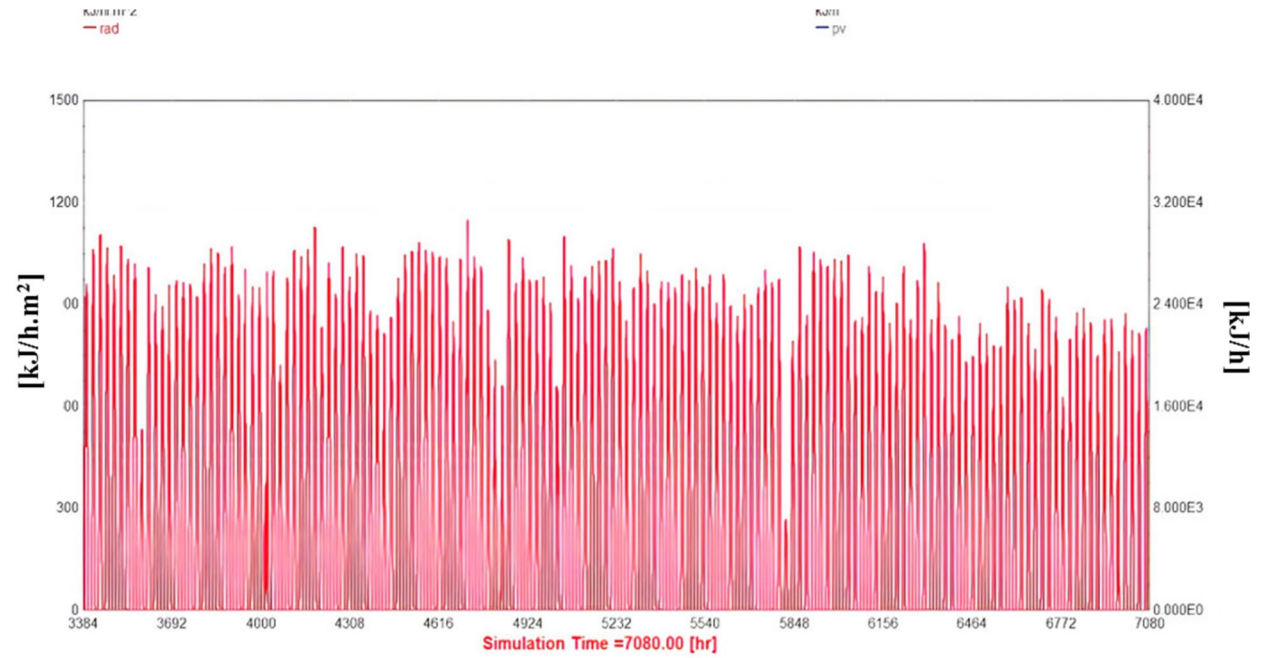
Also the performance of the same turbine in Kerman City was also checked (Fig. 12b), and it was found that the highest production power is $4.36 \times 10^{6,}$ and the highest efficiency occurred in early August, which is shown as 0.468. Also, when the efficiency reached its maximum value, the production power of the wind turbine was 2.28×10^6 W[37]. reported that urban areas have lower wind speeds due to obstructions such as buildings, while rural areas with more open spaces are more efficient for generating wind energy. Kerman, which has a
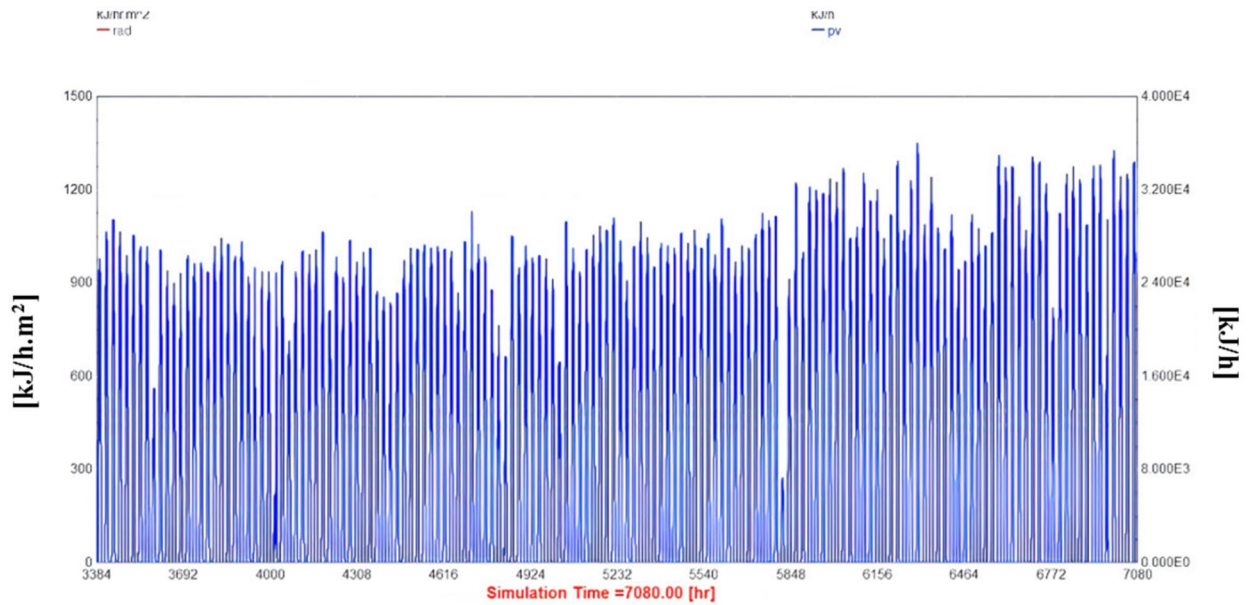
(a)

(b)
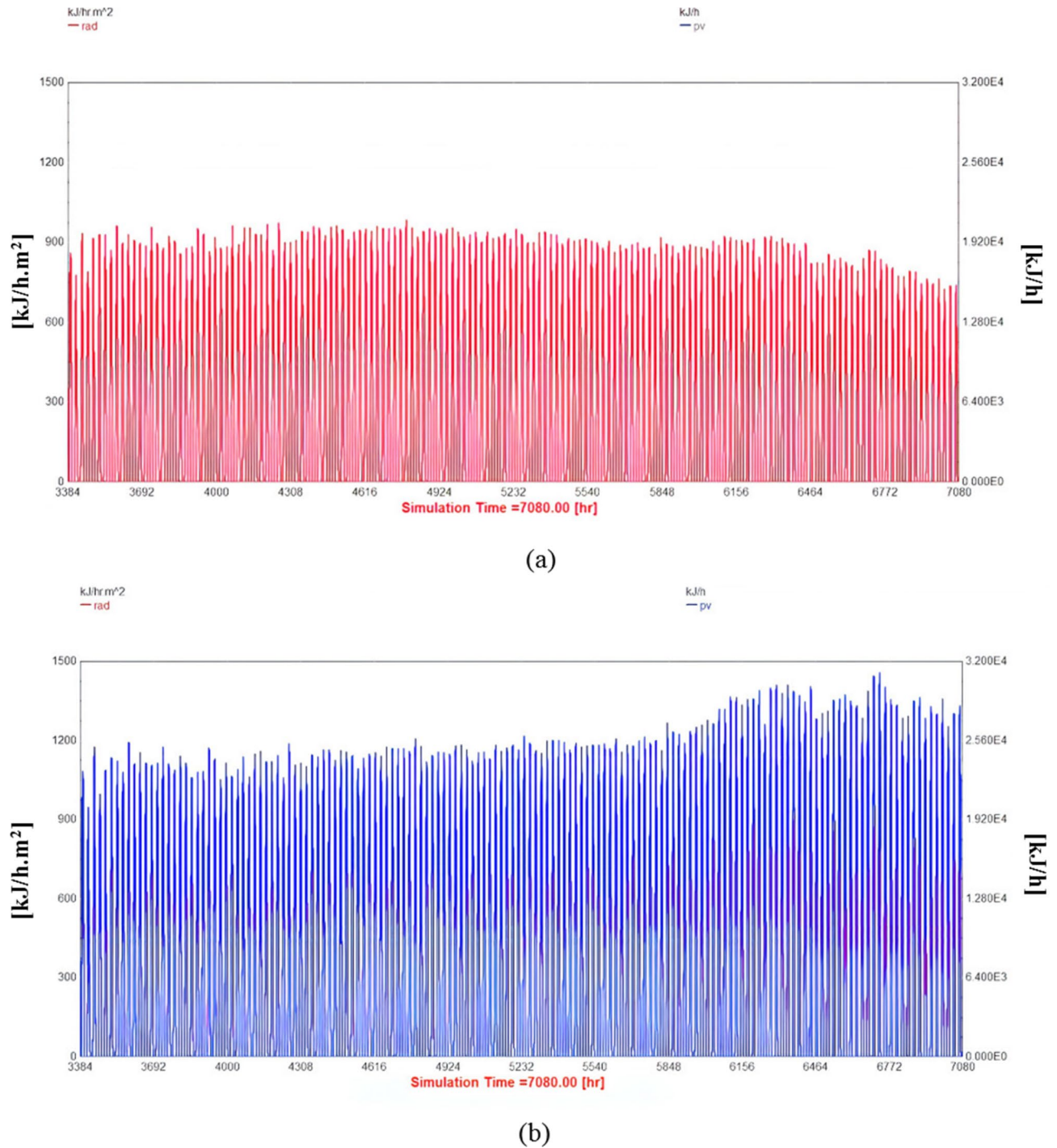
Fig. 9. Photovoltaic panel performance in Bushehr is (**a**) the amount of radiation to the surface of the panel and (**b**) the amount of power produced in the panel.

combination of urban and rural characteristics, showed moderate wind turbine performance in our study. This shows that while there are fewer obstacles in Kerman than in an urban environment, the wind speed is not as high as in coastal or rural environments.

After checking the data and graph of Shahrekord city (Fig. 12c), it was also determined that this city's highest turbine production power is 1.58×10^6 W, and its highest efficiency is 0.454 in early summer and June. It happened, also at the same time, the production efficiency was equal to its highest value, i.e., 1.58×10^6 w. higher altitudes with lower air densities generally result in lower wind energy output[38]. This can explain why Shahrekord, despite having favourable conditions for solar energy, showed lower wind turbine performance compared to Bushehr. The lower air density at Shahrekord's higher altitude reduces the kinetic energy available for conversion by the wind turbine.
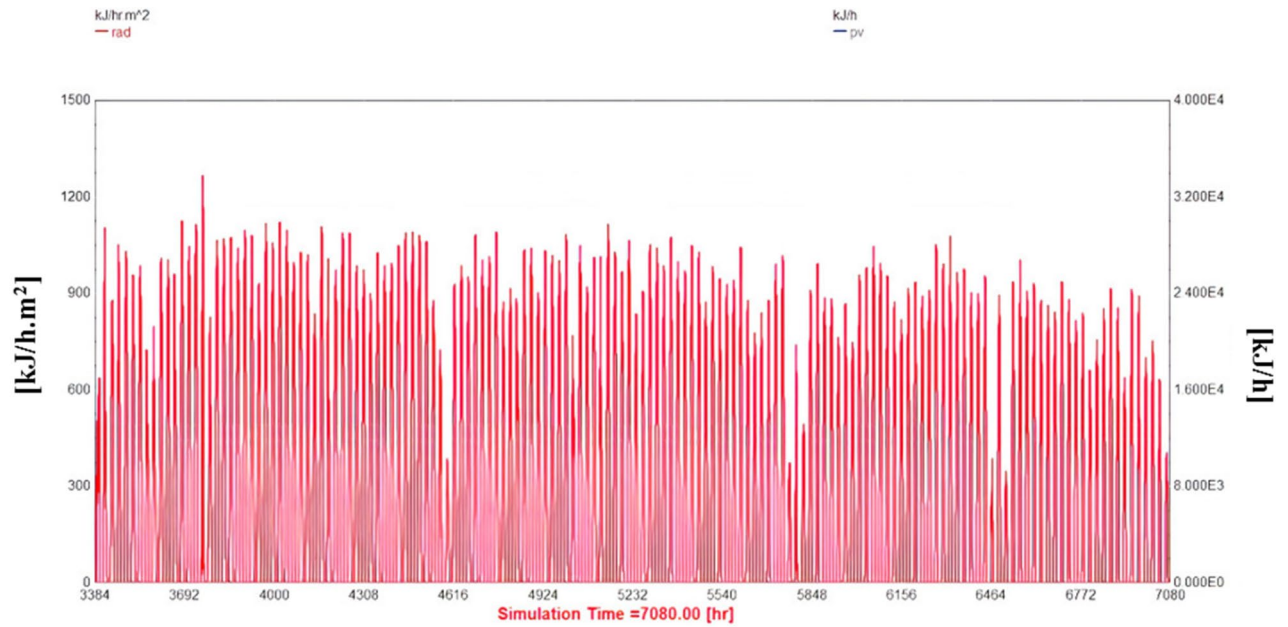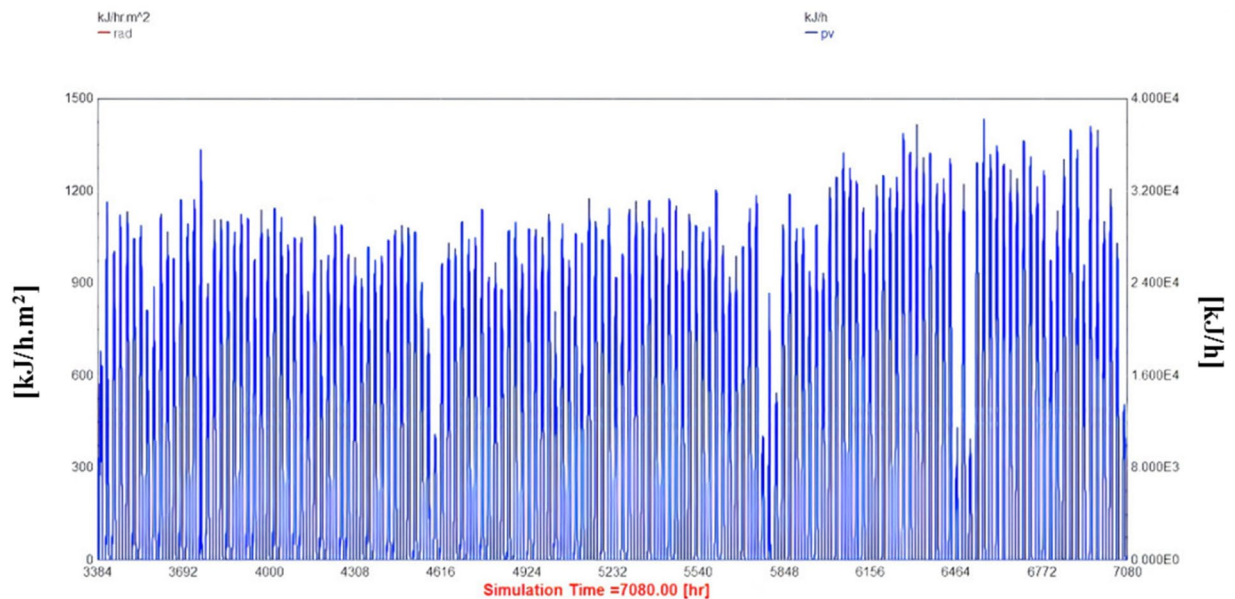
(a)

(b)

Fig. 10. Photovoltaic panel performance in Kerman is (**a**) the amount of radiation to the surface of the panel and (**b**) the amount of power produced in the panel.

The results of this analysis showed that the wind turbine efficiency in Bushehr city is better than that of the other two cities. According to the reports of[39], Iran has a very good potential for using wind energy. Wind energy potential in Iran is estimated to be about 6.5 GW to 15 GW. In fact, this amount is about 35% of the current electricity production in Iran[40]. in a study conducted on wind energy potential in India, it was found that coastal regions show high potential for wind energy generation due to their consistent wind speeds. This aligns with our findings in Bushehr, a coastal city with the highest wind turbine performance. Kumar et al. emphasize that the

(a)

(b)

Fig. 11. Photovoltaic panel performance in Shahrekord is (**a**) the amount of radiation to the surface of the panel and (**b**) the amount of power produced in the panel.

higher energy production in coastal areas is attributable to stable and higher wind speeds, which matches the wind profile observed in Bushehr.

Performance of photovoltaic panel and wind turbine

In this research, clean energy, such as solar and wind energy, has been used to reduce the costs and consequences caused by the use of fossil fuels. The two most important components that provide the energy consumption of this solar system's auxiliary system are the photovoltaic panel and the wind turbine. In fact, the amount of energy required for the auxiliary system, which is the thermal element inside the tank, has been provided by using photovoltaic panels and wind turbines. The performance of these two system components has been investigated

(a)

(b)

(c)
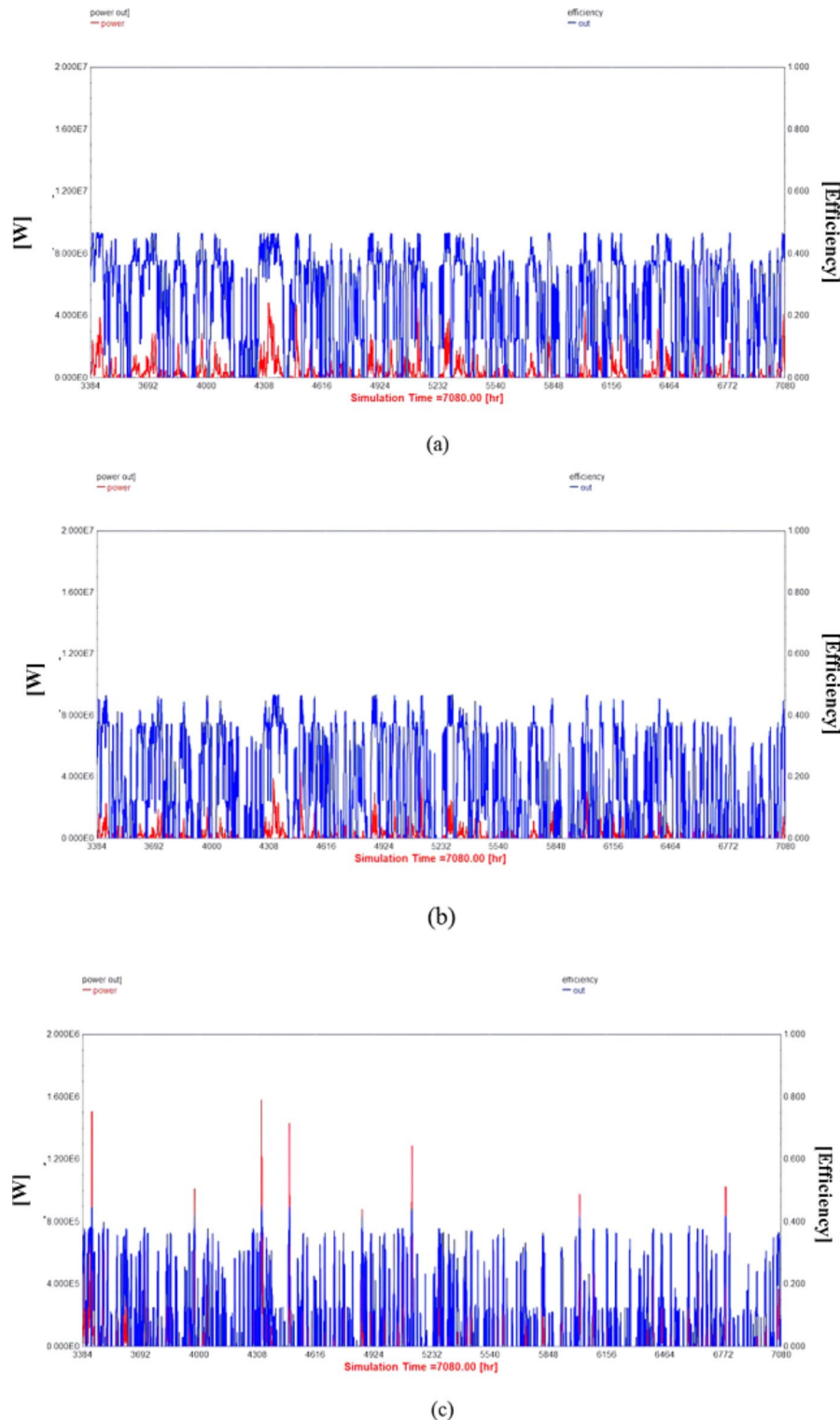
Fig. 12. Wind turbine performance in three cities (**a**) Bushehr (**b**) Kerman (**c**) Shahrekord.

in the three cities of Bushehr, Kerman, and Shahrekord. Table (7) shows the amount of power produced by photovoltaic panels and wind turbines during one year separately for each city.

According to the obtained data and the comparison of all three cities, it can be concluded that Shahrekord City has better potential in the field of photovoltaic panel installation than the other two cities. Bushehr had the highest and best performance in the field of wind turbine installation, considering that Bushehr is located on the southern coast of Iran. It is at the point where two hot and cold air flows meet. This intersection of hot and cold air flows can create strong and stable winds suitable for producing and using wind energy. Also,

Cities	photovoltaic panels produced power (W)	wind turbines produced power (W)
Bushehr	2.82×10^7	1.35×10^9
Kerman	3.11×10^7	6.37×10^8
Shahrekord	3.24×10^7	1.29×10^8

Table 7. Comparison of thermal power produced in the three cities of Bushehr, Kerman, and Shahrekord.

according to Table (7), The high potential of wind energy in Bushehr city is evident from the significant share of wind turbines. This is similar to the performance of other coastal areas around the world where wind energy is harnessed, such as coastal areas in Denmark and the UK (European Wind Energy Association, 2020). Also, according to the information obtained about the city of Kerman and the balanced share of wind and solar energy, it is clear that this city's conditions and geographical location are favourable for installing hybrid systems. Similar observations have been made in areas such as Texas, USA, where solar and wind energy are used (US Energy Information Administration, 2019). Also, according to the available data, the conditions of the city of Shahrekord were similar to areas with high solar radiation, such as Southern California and parts of Australia, which indicates the good potential of these cities in the use and installation of photovoltaic panels and solar systems (Agency between Renewable Energy International, 2018).

Thermal capacity of the tank

As it is clear from the graphs in Fig. (13), Bushehr experiences a relatively stable temperature due to its coastal location. The graph shows a steady trend in tank temperature with minimal fluctuations and temperature drops. The greatest drop in temperature occurs at the end of the summer season in September. This stability can be attributed to the marine climate, which moderates temperature fluctuations. However, Kerman and Shahrekord, which have a continental climate, show more obvious temperature changes. The greatest drop in temperature occurs at the end of spring and early summer (June and July). These fluctuations show the effect of higher altitudes and significant temperature differences between day and night.

Pipe

The pipes have the task of transferring hot water from the tank to the drying trays and transferring the heat required for the drying process to the drying trays. In this system, 200 m of copper pipes with a diameter of 1 cm were used. The graphs in Fig. (14) show the inlet temperature, outlet temperature, and internal energy change in pipes in all three cities.

As it is clear from these graphs, the inlet temperature value is higher than the outlet temperature value because the hot water enters the pipes at the same temperature, and after passing through all the trays and performing the drying process, it loses some temperature. Therefore, the water leaves the pipe at a lower temperature and returns to the cold part of the tank.

All three graphs (14a), (14b), and (14c) show the inlet temperature and the outlet temperature of the copper pipes connected to the drying tray. Also, the other part of this diagram determines the amount of internal energy changes inside these pipes during a specific time. According to these diagrams, the biggest change in the internal energy inside the pipes was about 1950 kJ/hr, and in this condition, the inlet temperature of the pipes was 55 ˚C, and the temperature of the water leaving the pipes was 52 ˚C. In fact, the water enters the cold part of the tank with 3 ˚C of energy loss compared to the initial temperature. Also, according to the obtained results, the average rate of the total energy entered into the pipe by the fluid flow was checked during one year, and it was determined that this value is equal to 3200 kJ/hr, and the average total internal energy changes inside the pipe during one year was equal to 478 kJ.

Of course, it should be noted that compared to other materials, copper pipes perform better in heat transfer applications. For example, although cheaper, aluminium tubes have lower thermal conductivity (237 W/mK), leading to slower heat transfer rates and longer, lower-quality drying processes. Studies have shown that systems that use copper pipes, compared to systems that use alternative materials, have higher thermal efficiency and produce a higher-quality product in a much shorter time[41].

Power output

This section discusses the power produced by the wind turbine and photovoltaic panel. It compares it with the amount of power consumed by the auxiliary system, which is the thermal element inside the tank. Table (8) shows the amount of power consumed by the auxiliary system (thermal element) and the amount of power produced by the system to supply the required energy of the thermal element.

As it is clear from the data in Table (2), the performance of wind turbines and photovoltaic panels in supplying energy to the auxiliary system (thermal element) has been very good. So, the amount of power produced by the system in all three cities was less than the power consumption of the auxiliary system during the specified period.

According to the comparison of the data in Table (2), it can be concluded that the solar system in Bushehr has performed better than the other two cities. Also, the auxiliary system in Shahrekord city has more consumption power than the other two cities.

Also, the analysis of energy contribution from photovoltaic panels and wind turbines based on the data presented in Table (7) and (8) indicates that in Bushehr, the PV and wind contributions are 2.05% and 97.95%. In Kerman, it is about 4.65% and 95.35%, and finally, in Shahrekord city is 20.08% and 79.92%, respectively. In

(a)

(b)
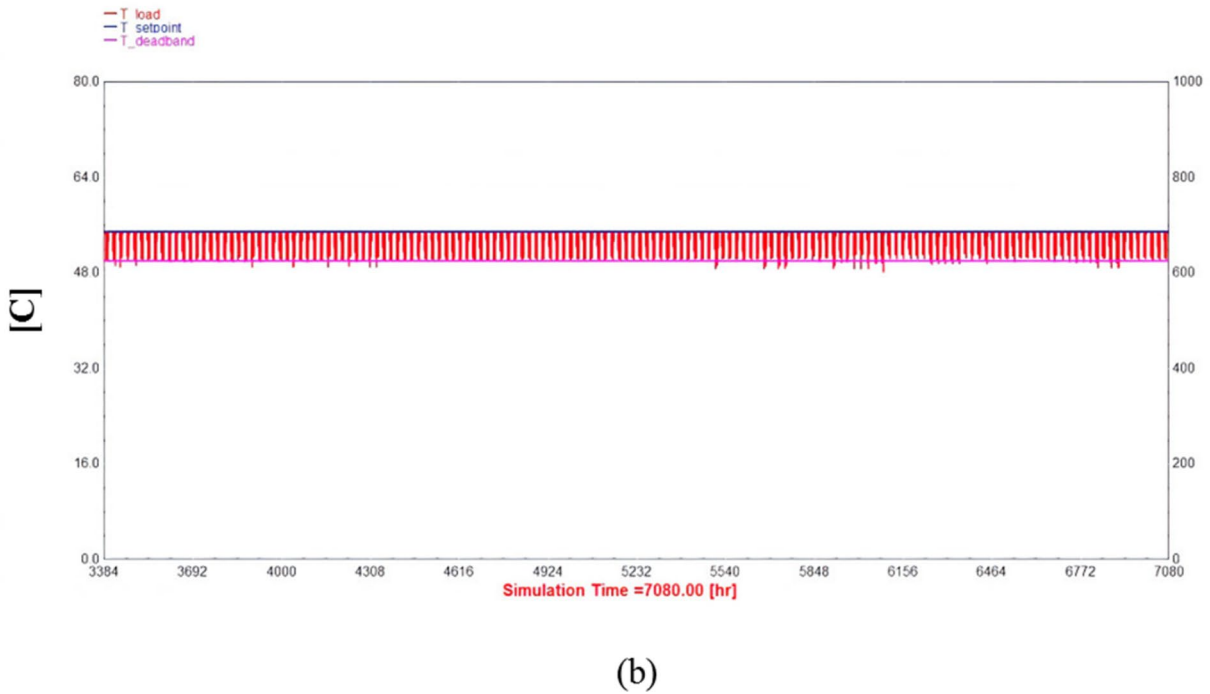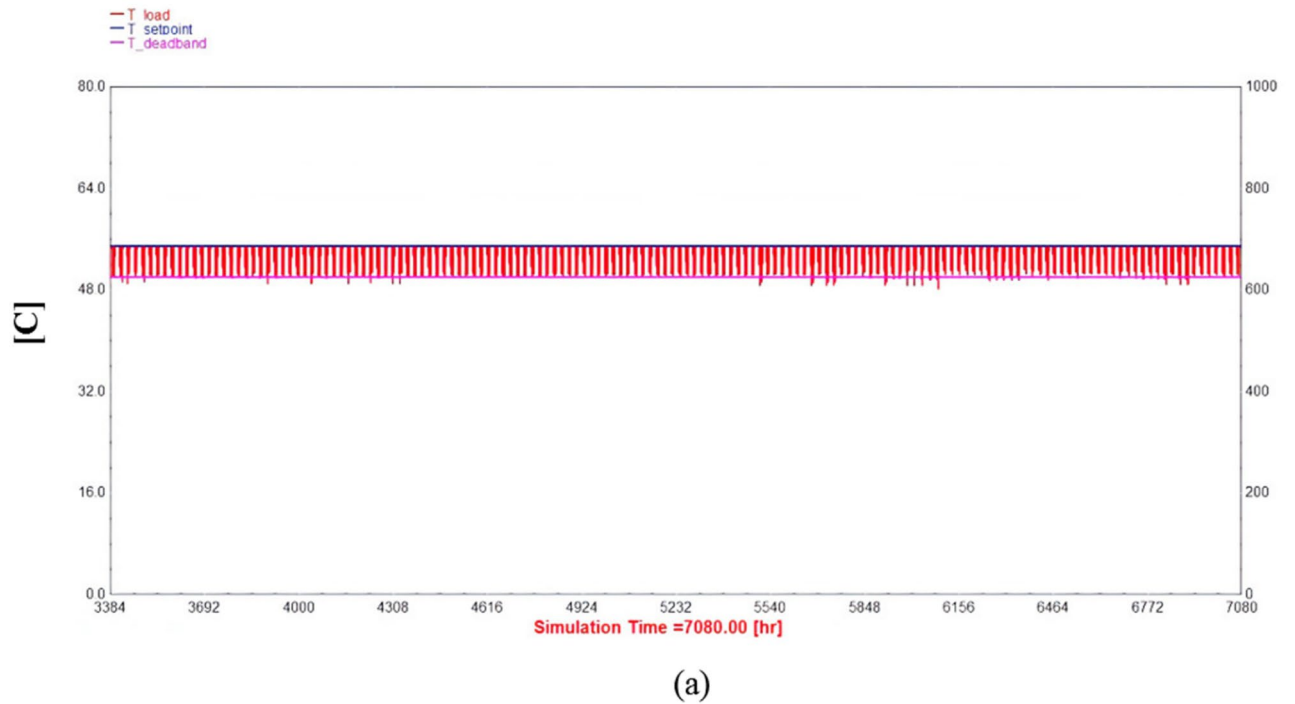
Fig. 13. tank thermal power in three cities (**a**) Bushehr (**b**) Kerman (**c**) Shahrekord.

order to determine the effectiveness of each energy source by cities, it can be seen that in Bushehr city, wind turbines are the main sources of energy for the auxiliary system, which provide 97.95% of the total energy, and this indicates a high energy potential of wind energy due to the coastal location of Bushehr. In the city of Kerman, the wind turbine plays the main role in supplying energy to the auxiliary system, and its amount is equal to 95.35% of the energy supplied, although, in Kerman, the percentage of energy supplied by PV panels is also higher than in Bushehr. However, it can concluded that Kerman has potential for both wind and solar energy. Also, in Shahrekord, PV panels have a significant share, which is equal to 20.08%, which reflects the very good conditions of this city in absorbing solar energy, although wind turbines still provide the majority of auxiliary
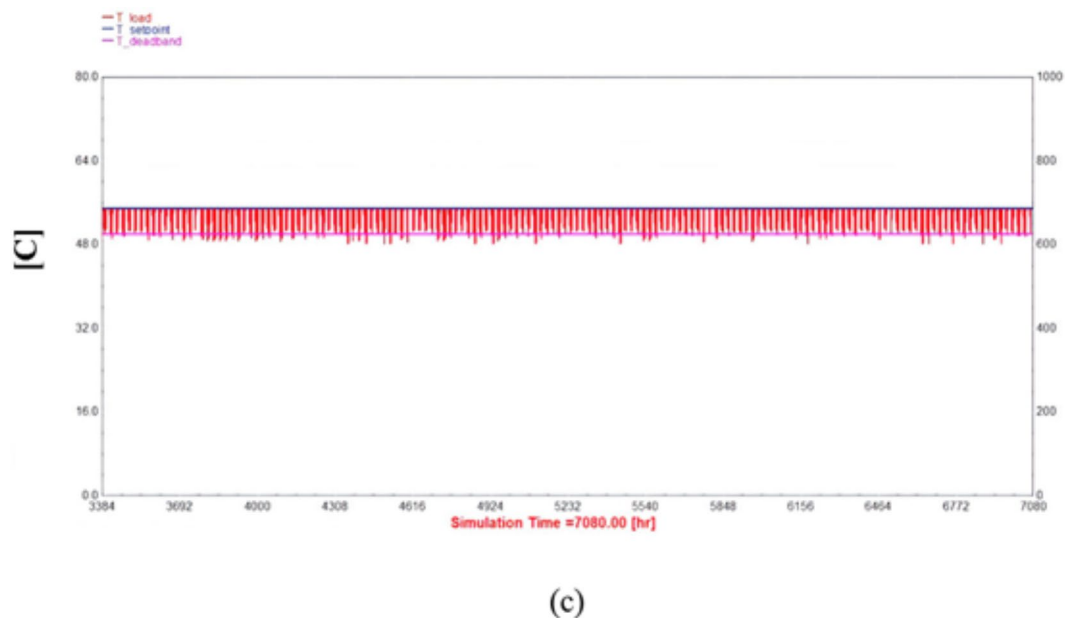
Figure 13. (continued)

system energy. From this information, it can be concluded that the geographical and climatic conditions of each city affect the performance and effectiveness of each energy source [42–44].

Hourly and yearly yield

Determining the system's yield is one of the most important parameters in the analysis of this solar system. Therefore, this section investigates the hourly and yearly yield of flat plate solar collectors and photovoltaic panels in the three mentioned cities. According to the graphs in Fig. (15), the highest yield of this system is related to Bushehr with 0.760, then Kerman with 0.755, and lastly, the lowest yield is related to Shahrekord city, which was equal to 0.738.

Also, according to the available results, the average yearly yield for Bushehr, Kerman, and Shahrekord cities is 0.301, 0.294, and 0.238, respectively. In fact, Bushehr has a higher efficiency than the other two cities due to its geographical location.

Comparison between the findings of this study and other solar drying methods

The drying process is critical in preserving agricultural products and increasing their shelf life, and various methods have been employed over the years. Traditional drying methods, such as open sun drying, are widely used due to their low cost and minimal environmental impact. However, these methods often suffer from significant drawbacks, including low control over the drying process, high exposure to contaminants, variable product quality, and slow drying rates. Solar hot plate dryers have been developed to address these issues, offering several advantages over traditional methods. As shown in Table (9), the solar hot plate dryer provides better control over the drying process, significantly reduces exposure to contaminants, and produces higher quality dried products at a faster rate. Although it incurs medium costs and has a variable capacity depending on the design, the benefits of using a solar hot plate dryer make it a viable alternative for improving the drying process in various settings[2,14,45].

Conclusion

In order to reduce post-harvest losses, one of the methods used to increase the quality of products and the shelf life of agricultural products is the drying process. This process consumes a lot of energy. In this research, a solar hot plate dryer system was designed and simulated in computer to reduce fossil fuel use and increase agricultural product shelf life. This system was tested in Iran in the three cities of Bushehr, Kerman, and Shahrekord. Also, this simulation was performed for the months of the year when more drying process is done (May 22 to October 23). Parameters investigated included total solar radiation, Solar water heating performance, Thermal capacity of the tank, energy changes in pipes, power output and Hourly and yearly yield. The results of this research showed that:

1. The highest amount of radiation is for Shahrekord City, and it was at the end of September (September 20), and was around 4540 kJ/m^{2}hr.
2. The solar collector and entire solar water heating system in Shahrekord has been better than that of the two other cities, and it has more favourable conditions.
3. Shahrekord has the best photovoltaic panel performance because of the amount of radiation absorbed to its surface and the amount of power produced in this city.
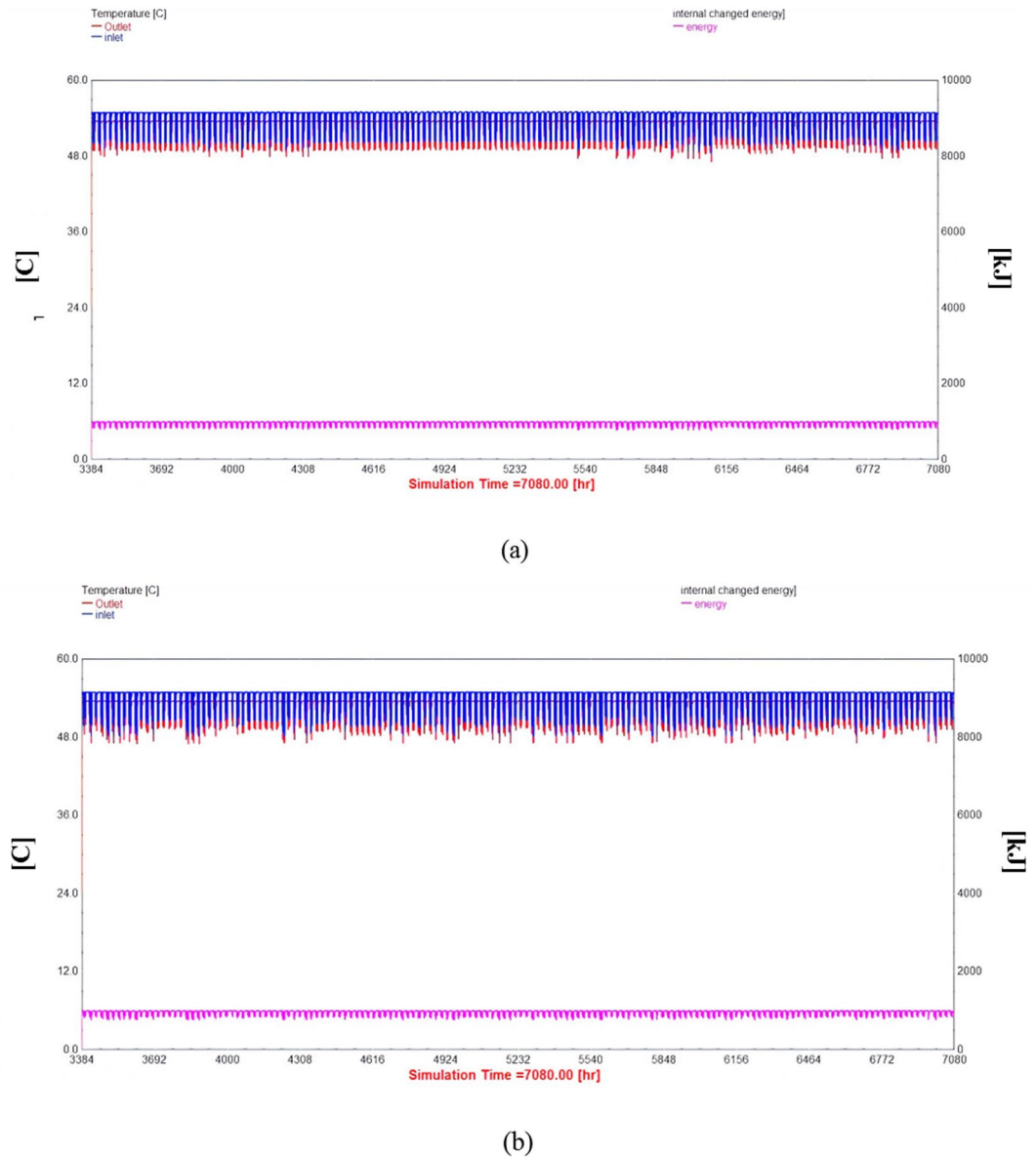
Fig. 14. Temperature and energy changes in pipes in three cities: (**a**) Bushehr, (**b**) Kerman, (**c**) Shahrekord.

4. Wind energy in Bushehr has better potential than Kerman and Shahrekord, and the highest power produced by the turbine in Bushehr was 4.86×10^6 W, also, the highest efficiency of the turbine in this city was about 0.468.

5. The highest efficiency of this system was related to Bushehr due to its geographical location, with a yield of 0.760.

6. The average yearly yield for Bushehr, Kerman, and Shahrekord was 0.301, 0.294, and 0.238, respectively.

Due to the results obtained from this simulation, it can be concluded that the potential of solar energy in Iran is substantial. Still, to realize this potential fully, further research is needed. Future studies should expand the research to include a wider range of cities and longer simulation periods to capture more comprehensive data. Also, specific recommendations for future research include:

- Improving Simulation Accuracy, for example, uses varying weather conditions and seasonal impacts to better predict the system's long-term performance.
- Exploring Hybrid Systems, for example, investigates integrating hybrid renewable energy systems, combining solar, wind, and other renewable sources to optimize energy production and system efficiency.
- Conducting a detailed economic analysis to assess the cost-effectiveness of implementing such systems on a larger scale. Additionally, evaluating the environmental benefits, including reductions in greenhouse gas emissions.
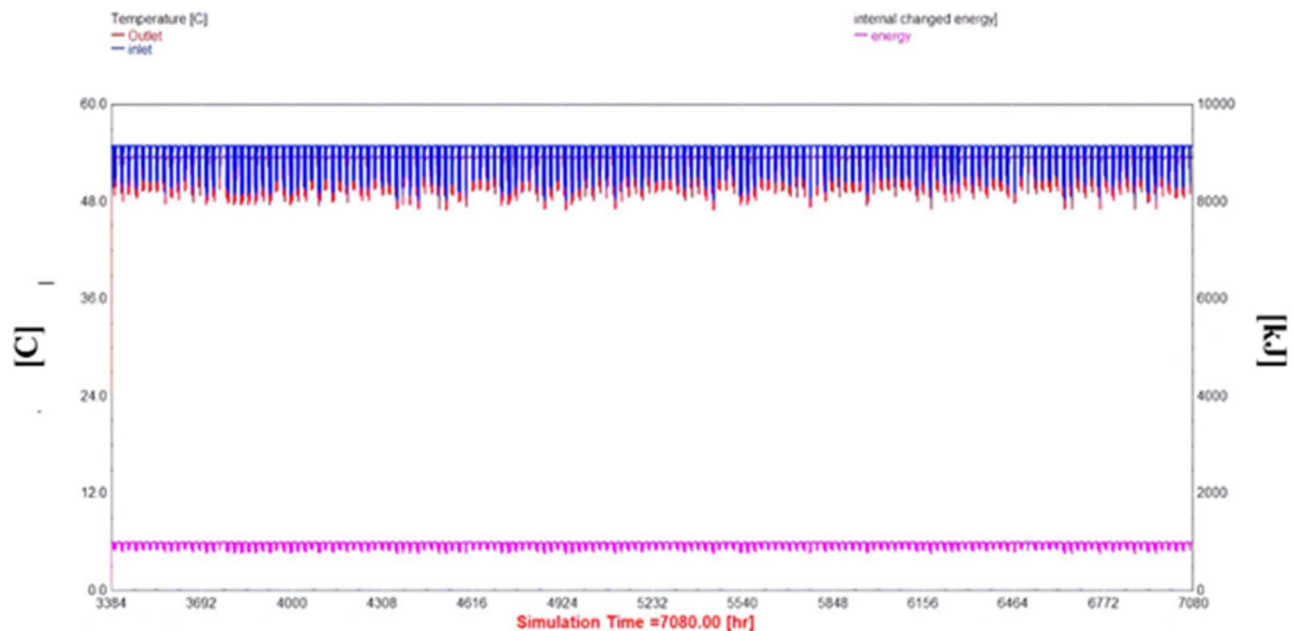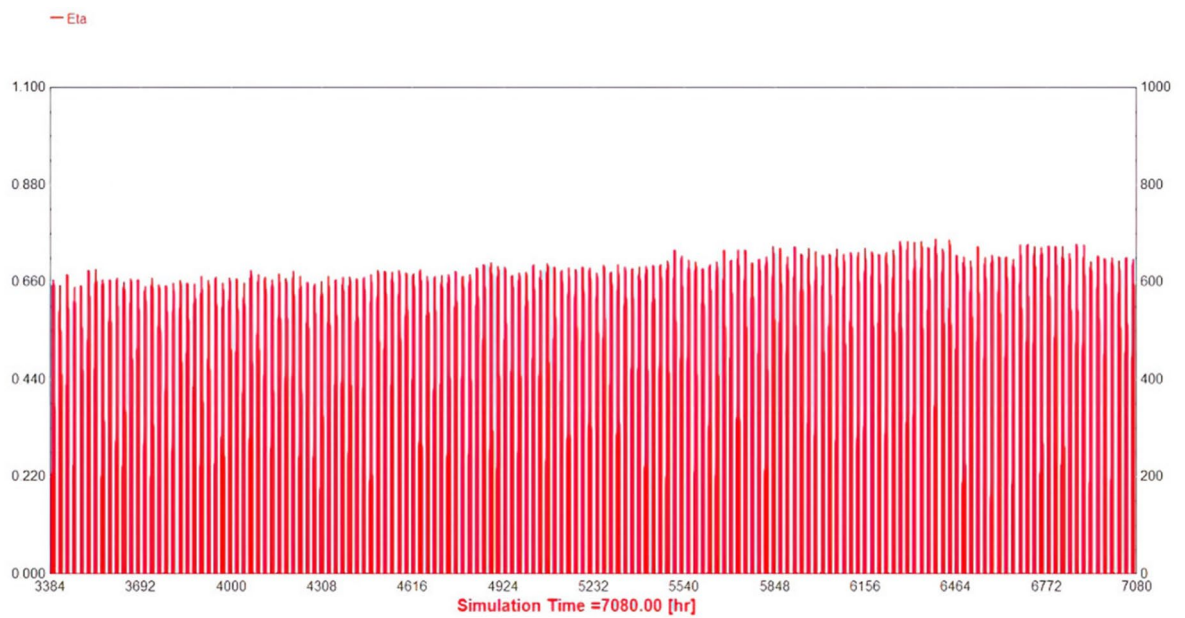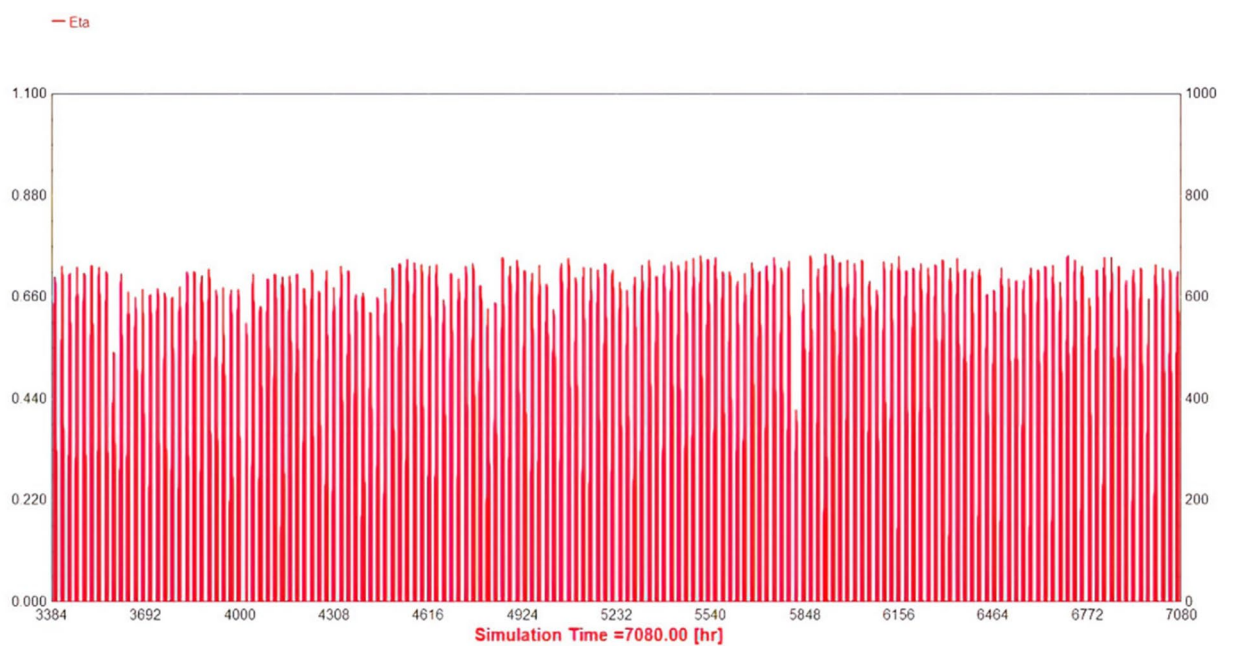
Figure 14. (continued)

Cities	Power output (W)	Power consumption of the auxiliary system (W)
Bushehr	1.37×10^9	4.34×10^7
Kerman	7.04×10^8	4.37×10^7
Shahrekord	1.61×10^8	4.42×10^7

Table 8. Comparing the power output of the system in the three cities of Bushehr, Kerman, and Shahrekord.

- Performing field trials in diverse geographic locations to validate simulation results and adapt the system design to real-world conditions.
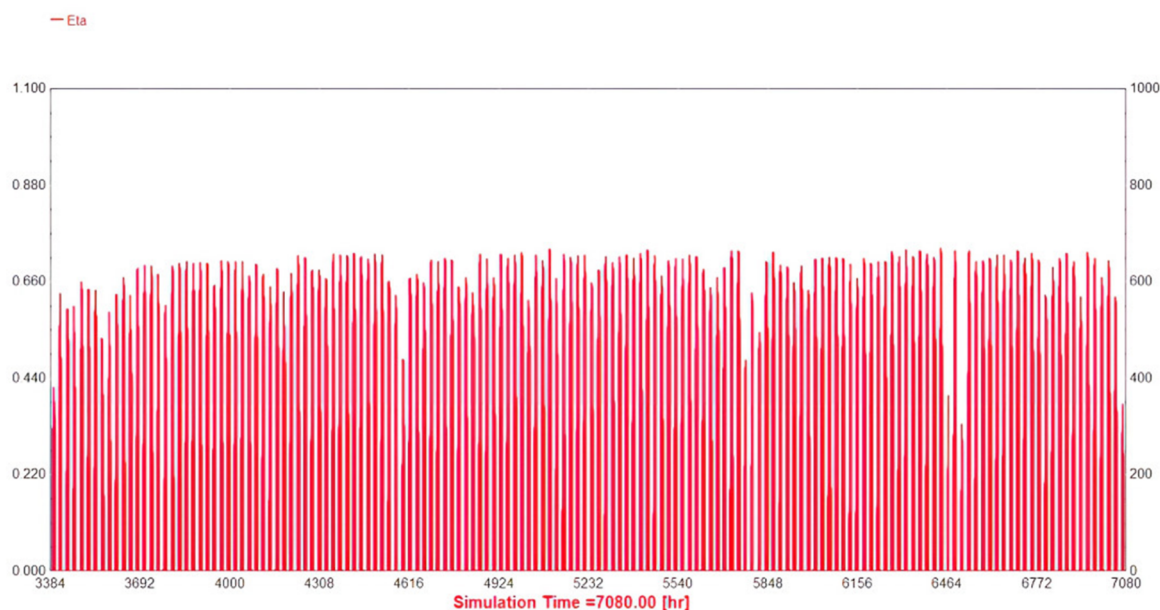
(a)

(b)

Fig. 15. yearly yield chart in three cities (**a**) Bushehr (**b**) Kerman (**c**) Shahrekord.

(c)

Figure 15. (continued)

Feature	Traditional drying methods	Solar hot plate dryer
Energy sources	Solar (direct sunlight)	Solar (indirect via solar collector, photovoltaic panel, wind turbines)
Control over the drying process	Low	High
Exposure to contaminants (% of product affected)	High (up to 30% exposed to envitonment such as rain, dust, pollution, insects)	Low (< 5%, enclosed system)
Final moisture content (%)	15-25%	8-12%
Cost	Low	Medium
Capacity	Low (1–3 kg/hour)	Variable (depends on design, usually 4–6 kg/hour)
Environmental impact	0 CO2 emissions (natural process)	Small emisions (~ 0.05 kg CO2/unit, due to the energy sources)
Drying rate	Slow (6–10 h)	Faster (2–4 h)

Table 9. Comparison of traditional drying methods with solar hot plate.

Data availability
The datasets generated and/or analyzed during the current study are available in Bahram Hosseinzadeh Samani repository [b.hosseinzadehsamani@gmail.com].

References
1. Saleem, M. S. et al. Design and optimization of hybrid solar-hydrogen generation system using TRNSYS. *Int. J. Hydrog. Energy*. **45**, 15814–15830 (2020).
2. Fudholi, A., Sopian, K., Ruslan, M. H., Alghoul, M. & Sulaiman, M. Y. Review of solar dryers for agricultural and marine products. *Renew. Sustain. Energy Rev.* **14**, 1–30 (2010).
3. Kannan, N. & Vakeesan, D. Solar energy for future world:-A review. *Renew. Sustain. Energy Rev.* **62**, 1092–1105 (2016).
4. Kabir, E., Kumar, P., Kumar, S., Adelodun, A. A. & Kim, K. H. Solar energy: potential and future prospects. *Renew. Sustain. Energy Rev.* **82**, 894–900 (2018).
5. Parsa, S. M. et al. First approach on nanofluid-based solar still in high altitude for water desalination and solar water disinfection (SODIS). *Desalination* **491**, 114592 (2020).
6. Alsehli, M. et al. Improving the performance of a hybrid solar desalination system under various operating conditions. *Process Saf. Environ. Prot.* **162**, 706–720 (2022).
7. Mustayen, A., Mekhilef, S. & Saidur, R. Performance study of different solar dryers: a review. *Renew. Sustain. Energy Rev.* **34**, 463–470 (2014).

8. Samani, B. H., Lorigooini, Z., Zareiforoush, H. & Jafari, S. Effect of ultrasound and infrared drying methods on quantitative and qualitative characteristics of Satureja Bachtiarica essential oil. *J. Essent. Oil Bearing Plants*. **20**, 1196–1208 (2017).
9. Wang, A. M. S. E. C. et al. *INMATEH-Agricultural Eng*. **54**, 55–62 (2018).
10. Abur, B. T., Dandakouta, H. & Ejilah, R. Modeling and Simulation of an Indirect Natural Convection Solar Dryer with Thermal Storage Bed. *Int. J. Comput. Netw. Inform. Secur*. **8**, 24–42 (2020).
11. Samani, B. H. et al. Development and optimization of the new ultrasonic-infrared-vacuum dryer in drying Kelussia odoratissima and its comparison with conventional methods. *Ind. Crops Prod*. **123**, 46–54 (2018).
12. Ebuy, H. T. *Simulation of Solar Cereal Dryer Using TRNSYS* (Addis Ababa University, 2007).
13. Xie, Z., Gong, Y., Ye, C., Yao, Y. & Liu, Y. Numerical analysis and optimization of solar-assited heat pump drying system with waste heat recovery based on TRNSYS. *Processes* **9**, 1118 (2021).
14. Kumar, M., Sansaniwal, S. K. & Khatak, P. Progress in solar dryers for drying various commodities. *Renew. Sustain. Energy Rev*. **55**, 346–360 (2016).
15. Mohammed, S. A. et al. Optimized solar food dryer with varied air heater designs. *Case Stud. Therm. Eng*. **53**, 103961 (2024).
16. Lamrani, B., Khouya, A. & Draoui, A. Energy and environmental analysis of an indirect hybrid solar dryer of wood using TRNSYS software. *Sol. Energy*. **183**, 132–145 (2019).
17. Seveda, M. & Jhajharia, D. Design and performance evaluation of solar dryer for drying of large cardamom (Amomum Subulatum). *J. Renew. Sustain. Energy* **4** (2012).
18. Zomorodian, A. & Dadashzadeh, M. Indirect and mixed mode solar drying mathematical models for sultana grape. (2009).
19. Fadhel, M., Abdo, R. A., Yousif, B., Zaharim, A. & Sopian, K. in *Proceedings of the 6th IASME/WSEAS International Conference on Energy and Environment (EE 2011)*. (University of Southern Queensland).
20. Khalil, A., Khaira, A. M., Abu-Shanab, R. H. & Abdelgaied, M. A comprehensive review of advanced hybrid technologies that improvement the performance of solar dryers: Photovoltaic/thermal panels, solar collectors, energy storage materials, biomass, and desalination units. *Sol. Energy*. **253**, 154–174 (2023).
21. Reyes, A., Mahn, A. & Vásquez, F. Mushrooms dehydration in a hybrid-solar dryer, using a phase change material. *Energy. Conv. Manag*. **83**, 241–248 (2014).
22. Ahmadi, A. et al. Energy, exergy, and techno-economic performance analyses of solar dryers for agro products: a comprehensive review. *Sol. Energy*. **228**, 349–373 (2021).
23. Philip, N., Duraipandi, S. & Sreekumar, A. Techno-economic analysis of greenhouse solar dryer for drying agricultural produce. *Renew. Energy*. **199**, 613–627 (2022).
24. Oueslati, F. Hybrid renewable system based on solar wind and fuel cell energies coupled with diesel engines for Tunisian climate: TRNSYS simulation and economic assessment. *Int. J. Green Energy*. **18**, 402–423 (2021).
25. Ayompe, L., Duffy, A., McCormack, S. & Conlon, M. Validated TRNSYS model for forced circulation solar water heating systems with flat plate and heat pipe evacuated tube collectors. *Appl. Therm. Eng*. **31**, 1536–1542 (2011).
26. Alshibil, A. M., Farkas, I. & Víg, P. Multi-aspect approach of electrical and thermal performance evaluation for hybrid photovoltaic/thermal solar collector using TRNSYS tool. *Int. J. Thermofluids*. **16**, 100222 (2022).
27. Karassik, I. J. *Pump handbook*. (2001).
28. Ołtarzewska, A. & Krawczyk, D. A. The use of solar collectors in domestic Hot Water systems in Central and Eastern European Countries: Simulation in TRNSYS. *Environ. Clim. Technol*. **27**, 243–253 (2023).
29. Kakaç, S., Yener, Y. & Naveira-Cotta, C. P. *Heat Conduction* (CRC, 2018).
30. White, F. M., Ng, C. & Saimek, S. *Fluid mechanics*. (McGraw-Hill, cop., 2011).
31. Besarati, S. M., Padilla, R. V., Goswami, D. Y. & Stefanakos, E. The potential of harnessing solar radiation in Iran: Generating solar maps and viability study of PV power plants. *Renew. Energy*. **53**, 193–199 (2013).
32. Ghasemi, G., Noorollahi, Y., Alavi, H., Marzband, M. & Shahbazi, M. Theoretical and technical potential evaluation of solar power generation in Iran. *Renew. Energy*. **138**, 1250–1261 (2019).
33. Enjavi-Arsanjani, M., Hirbodi, K. & Yaghoubi, M. Solar energy potential and performance assessment of CSP plants in different areas of Iran. *Energy Procedia*. **69**, 2039–2048 (2015).
34. Rezapour, S. et al. Dynamic simulation and ranking of using residential-scale solar water heater in Iran. *J. Environ. Eng. Landsc. Manage*. **30**, 30–42 (2022).
35. Akikur, R. K., Saidur, R., Ping, H. W. & Ullah, K. R. Comparative study of stand-alone and hybrid solar energy systems suitable for off-grid rural electrification: a review. *Renew. Sustain. Energy Rev*. **27**, 738–752 (2013).
36. Hasanuzzaman, M. et al. Energy savings in the combustion based process heating in industrial sector. *Renew. Sustain. Energy Rev*. **16**, 4527–4536 (2012).
37. Ali, B. et al. A comparative study to analyze wind potential of different wind corridors. *Energy Rep*. **9**, 1157–1170 (2023).
38. Jouchi, A. A., Pourrajabian, A., Rahgozar, S. & Dehghan, M. Performance appraisal of a small wind turbine under the use of three rotor hub configurations. *Clean Technol. Environ. Policy*. **25**, 1509–1523 (2023).
39. Moghaddam, N. B., Mousavi, S. M., Nasiri, M., Moallemi, E. A. & Yousefdehi, H. Wind energy status of Iran: evaluating Iran's technological capability in manufacturing wind turbines. *Renew. Sustain. Energy Rev*. **15**, 4200–4211 (2011).
40. Kumar, J. C. R., Kumar, D. V. & Majid, M. Wind energy programme in India. *Energy Environ*. **30**, 1135–1189 (2019).
41. Patel, A. K. Comparative analysis of solar heaters and heat exchangers in residential water heating. *Int. J. Sci. Res. Archive*. **9**, 830–843 (2023).
42. Hosseini, S. E., Andwari, A. M., Wahid, M. A. & Bagheri, G. A review on green energy potentials in Iran. *Renew. Sustain. Energy Rev*. **27**, 533–545 (2013).
43. Vahdatpour, S., Behzadfar, S., Siampour, L., Veisi, E. & Jahangiri, M. Evaluation of off-grid hybrid renewable systems in the four climate regions of Iran. *J. Renew. Energy Environ*. **4**, 61–70 (2017).
44. Alamdari, P., Nematollahi, O. & Alemrajabi, A. A. Solar energy potentials in Iran: a review. *Renew. Sustain. Energy Rev*. **21**, 778–788 (2013).
45. Prakash, O., Laguri, V., Pandey, A., Kumar, A. & Kumar, A. Review on various modelling techniques for the solar dryers. *Renew. Sustain. Energy Rev*. **62**, 396–417 (2016).

Acknowledgements

Author contributions

Kimia Taki: Simulation; wrote the paper.Bahram Hosseinzadeh Samani: Supervisor; wrote the paper.Mahsa Forouzandeh and Zahra Shafiee: revise the paper, Simulation assistant.

Declarations

Competing interests
The authors declare no competing interests.

Consent for publication
All authors have agreed to publish this manuscript.

Additional information
Correspondence and requests for materials should be addressed to B.H.S.

Reprints and permissions information is available at www.nature.com/reprints.

Publisher's note Springer Nature remains neutral with regard to jurisdictional claims in published maps and institutional affiliations.